Structural Engineering and Mechanics, *Vol. 58, No. 2 (2016) 347-378*
DOI: http://dx.doi.org/10.12989/sem.2016.58.2.347

The influence of the initial stresses on Lamb wave dispersion in pre-stressed PZT/Metal/PZT sandwich plates

Ilkay Kurt*[1], Surkay D. Akbarov[1,2a] and Semih Sezer[1b]

[1]*Department of Mechanical Engineering, Yildiz Technical University, Yildiz Campus, 34349, Besiktas, Istanbul, Turkey*
[2]*Institute of Mathematics and Mechanics of the National Academy of Sciences of Azerbaijan, 37041, Baku, Azerbaijan*

(Received July 14, 2015, Revised January 15, 2016, Accepted February 2, 2016)

Abstract. Within the scope of the plane-strain state, by utilizing the three-dimensional linearized theory of elastic waves in initially stressed piezoelectric and elastic materials, Lamb wave propagation and the influence of the initial stresses on this propagation in a sandwich plate with pre-stressed piezoelectric face and pre-stressed metal elastic core layers are investigated. Dispersion equations are derived for the extensional and flexural Lamb waves and, as a result of numerical solution to these equations, the corresponding dispersion curves for the first (fundamental) and second modes are constructed. Concrete numerical results are obtained for the cases where the face layers' materials are PZT-2 or PZT-6B, but the material of the middle layer is Steel (St) or Aluminum (Al). Sandwich plates PZT-2/St/PZT-2, PZT-2/Al/PZT-2, PZT-6B/St/PZT-6B and PZT-6B/Al/PZT-6B are examined and the influence of the problem parameters such as piezoelectric and dielectric constants, layer thickness ratios and third order elastic constants of the St and Al on the effects of the initial stresses on the wave propagation velocity is studied.

Keywords: extensional and flexural Lamb waves; initial stresses; wave dispersion; piezoelectric material; sandwich plate; third order elastic constants

1. Introduction

The study of coupling electro-mechanical problems related to the dynamics of structures containing piezoelectric and elastic layers has great significance not only in the theoretical sense, but also in the application sense. The reasons for this are the many applications of these types of structures in almost all branches of modern industry such as aerospace, marine, mechanical engineering, acoustoelectric devices etc. Among these dynamic problems, a special place is occupied by problems regarding the wave propagation, especially near-surface and Lamb wave propagation, of which, out of the aforementioned structures are sandwich plates which are widely used in many technical applications. This is because Lamb waves in the sandwich or other type of

∗Corresponding author, Ph.D. Student, E-mail: ikurt@yildiz.edu.tr
[a]Professor, E-mail: akbarov@yildiz.edu.tr
[b]Associate Professor, E-mail: sezer@yildiz.edu.tr

http://www.techno-press.org/?journal=sem&subpage=8 ISSN: 1225-4568 (Print), 1598-6217 (Online)

layered structural elements made of piezoelectric and elastic materials can be used to obtain reliable information on the carrying work capacity of the elements of constructions (see Ng 2015, Wang *et al*. 2015 and others). For instance, Lamb waves can propagate long distances between two top and bottom surfaces in thin-wall structures, and with the ability of carrying information about the material, it has great importance for non-destructive testing and structural health monitoring in plate-like structures.

It is evident that under the foregoing applications, it is necessary to have sufficient information and knowledge about the influence of the piezoelectric layers mounted on the surface of the tested structural elements on the wave propagation (or dispersion) in this element. It is also evident that this type of information can be obtained by theoretical investigations carried out on the wave propagation in the system consisting of a piezoelectric covering layer + elastic half-plane (for the near surface waves) and in the sandwich plate consisting of the piezoelectric face and elastic core layers (for the Lamb waves). Moreover, the study of acoustoelastic waves in the layered systems with piezoelectric layers is required by the current importance, from the point of view of both fundamental research and applications, in various acoustoelastic devices.

Thus, according of the foregoing discussions, we can conclude that the subject of the present paper which relates to the study of Lamb waves in a sandwich plate consisting of piezoelectric face and elastic metal core layers with static initial stresses is very important not only in the theoretical sense, but also in the application sense. It should be noted that the initial stresses are characteristic reference properties of the layered structures. These stresses can be caused by the compounding procedure of these structures. They can also appear as a result of environmental conditions (for instance, temperature). Moreover, static stresses caused by exploitational forces can also be taken as the initial stresses with respect to those caused with additional small dynamic perturbations. Consequently, there exist a lot of reasons for the appearance of the initial stresses, and study as to how these stresses act on the wave propagation velocities also has importance. For estimation of the significance of the investigation carried out in the present paper, we consider a brief review of related works. We begin with a paper by Loja *et al*. (2013) in which the static and free vibration behavior of functionally graded sandwich plates with piezoelectric outer layers was examined. Under this examination, the corresponding third order refined plate theory is developed and it is established that the model developed is quite adequate to describe the static behavior of the piezoelectric layered structures.

Bassiouny (2012) studied the one-dimensional dynamic problem related to the coupled termo piezoelectricity for the sandwich structure with piezoelectric layers. The generalized termo-piezoelectric-elasticity relations are used and it is assumed that all sought values depend only on the coordinate directed along the thickness of the plate. For solution to the corresponding mathematical problems, the Laplace transformation with respect to time is employed. It is established that using the generalized termo-piezoelectric-elasticity relations, the heat waves, as in generalized termo-elasticity, propagate with finite speed.

Azrar *et al*. (2008) studied nonlinear vibration of the sandwich beam with piezoelectric face layers and with initial imperfection. The beam is subjected to axial displacement and active voltage which is generated by the top and the bottom piezoelectric layers. Obtained results take into consideration the piezoelectricity, the beam initial imperfection and the axial load effects and can be easily used in order to predict the nonlinear static and dynamic behaviours of sandwich beams with layer actuators. The study is made within the scope of the Bernoulli-Euler beam theory and von-Karmen type non-linearity for beams with initial imperfection.

In a paper by Jin *et al*. (2002), this type of near-surface wave dispersion is examined for the

system of the piezoelectric covering layer made of PZT-4 and the half-plane made of Aluminum. The results obtained in the paper by Jin *et al*. (2002) is developed in a work by Akbarov *et al*. (2014) for other types of piezoelectric and half-plane materials. Moreover, in the work by Akbarov *et al*. (2014) the influence of the initial stresses in the constituents on the near-surface dispersion is studied.

Pang *et al*. (2008) studied Rayleigh type surface waves for the system consisting of the covering layer made of PZT-4 and piezomagnetic half-space. It should be noted that the results obtained in the works by Pang *et al*. (2008) and Akbarov *et al*. (2014), which relate to the case where the covering layer material is PZT-4, agree with each other in the qualitative sense.

Note that in all the investigations reviewed above (except the work by Akbarov *et al*. 2014), it is assumed that there are no initial stresses in the constituents of the layered systems with piezoelectric constituents. However, up to now, a certain number of investigations have been made related to the influence of the initial stresses on the wave propagation in the layered systems, containing elastic constituents only. For instance, a paper by Gupta *et al*. (2012) deals with the study of torsional surface waves in the system consisting of homogeneous covering layer with finite thickness and an initially stressed heterogeneous half-space. Equations of motion of the layer are written within the scope of the classical linear theory of elastic waves, however, equations of motion of the pre-stressed inhomogeneous half plane are written within the scope of Biot's (1965) incremental deformation theory. Numerical results on the influence of the initial stresses in the half-space on the dispersion curves are presented and discussed. Moreover, in the papers by Akbarov *et al*. (2008, 2011), Lamb wave dispersion in the sandwich plate made of highly-elastic compressible materials is investigated and it is assumed that the layers of the plate have initial finite strains. The problem is studied by utilizing the first version of the initial deformation theory of the three-dimensional linearized theory of elastic waves in initially stressed bodies (Guz 2004). The results obtained in the papers by Akbarov *et al*. (2008, 2011, 2014) were also detailed in a monograph by Akbarov (2015).

Thus, it follows from the foregoing review that up to now there have been no investigations related to the study of Lamb wave propagation in the sandwich plate with piezoelectric face and elastic core layers. Therefore in the present paper the first attempt is made in this field and Lamb wave propagation (dispersion) in the sandwich plate with initial stresses is investigated utilizing the three-dimensional linearized theory of elastic waves in electro-elastic bodies with initial stresses. Concrete numerical results, i.e., dispersion curves are presented for the case where the face layers' materials are PZT-2 and PZT-6B, and the material of the core layer is Steel (St) or Aluminum (Al). Mechanical relations for the materials Al and St are given through the Murnaghan potential to take into consideration the effect of the third order elastic constants of these materials on the behavior of the Lamb wave propagation. Consequently, numerical investigations are examined for the PZT-2/St/PZT-2, PZT-2/Al/PZT-2, PZT-6B/St/PZT-6B and PZT-6B/Al/PZT-6B sandwich plates and the influence of the problem parameters such as piezoelectric and dielectric constants, layer thickness ratios and third order elastic constants of the St and Al on the effects of the initial stresses on the wave propagation velocity is studied.

2. Formulation of the problem

Consider the Lamb wave propagation in a sandwich plate consisting of an initially stressed core-middle metal elastic layer with thickness $2H_{core}$ and of two initially stressed piezoelectric face

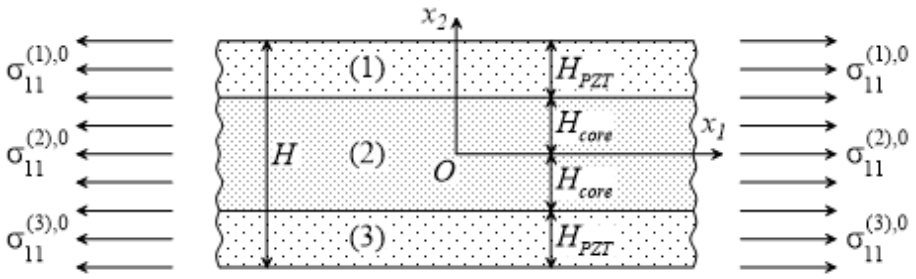

Fig. 1 The geometry of the sandwich plate consisting of the pre-stressed piezoelectric face layers and pre-stressed middle layer

layers each of which has a thickness H_{PZT} and each of which is made from the same material. With the mid-plane of the core layer of the plate, we associate the Cartesian coordinate system $Ox_1x_2x_3$ (Fig. 1) and the position of the points of the constituents we determine by the Lagrange coordinates in this system. Assume that the layers of the plate have infinite length in the directions of the Ox_1 and Ox_3 axes (the coordinate axis Ox_3 is perpendicular to the figure plane and therefore is not shown in Fig. 1). Below, the values relating to the upper and lower face layers will be denoted by the indices (1) and (3), respectively, while the values relating to the core layer will be denoted with the upper index (2). Moreover, the values relating to the initial (residual) stresses will be denoted by the upper indices $(m),0$ where m=1,2 and 3.

We employ the second version of the small initial deformation version of the three-dimensional linearized theory of elastic waves in initially stressed elastic and piezoelectric bodies (TDLTEPWISB) (see the references Guz (1999, 2004), Yang (2005) in which this version is called the linearized wave propagation theory in initially stressed piezoelectric materials) for investigation of the dispersion of Lamb waves in the foregoing initially stressed sandwich plate. According to this version of the TDLTEWISB, the initial stresses in the bodies under consideration are determined within the scope of the classical linear theory of electro-elasticity. Taking the foregoing assumption into account, we consider the case where the initial stresses in the layers of the plate are homogeneous and determined as follows.

$$\sigma_{11}^{(m),0} = const_m \neq 0\,,\ \sigma_{12}^{(m),0} = \sigma_{22}^{(m),0} = 0\,,\ m = 1,2,3\,. \tag{1}$$

According to the electro-elasticity relations for the piezoelectric materials, which will be given below, in the initial state in the case where the piezoelectric material is polled along the direction of the Ox_2 axis (Ox_1 axis), the component $E_2^{(m)0}$ ($E_1^{(m)0}$) of the electric field vector and the component $D_2^{(m)0}$ ($D_1^{(m)0}$) of the electric displacement vector differ from zero and are determined through the initial stresses in (1) and the elastic, piezoelectric and dielectric constants of the corresponding material. However, the components of the electric field vectors and electric displacement vectors do not enter into the considered version of the linearized equations of motion of electro-elasticity for the piezoelectric materials. Therefore we do not give here the expression for calculation of the values of these quantities. Note that these expressions can be established by the reader with the use of the electro-elasticity relations which will be given below.

We note that the initial stresses determined by the expressions in (1) can be caused by the uniformly distributed static normal forces acting simultaneously at the ends of the sandwich plate,

i.e., at $x_1 \to \infty$ and $x_1 \to +\infty$. This is because, according to the Saint-Venant principle, the inhomogeneity of the stresses at the near vicinity of the ends $|x_1| \to \infty$ disappears and the stresses become homogeneous as formulated in (1). Consequently, the appearance of the homogeneous initial stresses in (1) is sufficiently real and can be applied at a distance, with the order of the plate thickness, from the ends at which the aforementioned normal forces act. However, in this case the stresses related to the face and core layers are connected with each other through a certain expression which can be easily determined (see, for instance, Akbarov 2015). Moreover, the initial stresses in (1) can appear in the following manner: first each layer is statically loaded at their ends with normal forces with intensity $\sigma_{11}^{(1),0}$ for the face layers, and with intensity $\sigma_{11}^{(2),0}$ for the core layer and then these layers are connected with each other. Consequently, each of the foregoing cases related to the appearance of the initial stresses in (1) is real and both the formulation of the problem and method of solution of this problem are acceptable for each of the foregoing cases.

Thus, within the scope of the foregoing assumption and notation we write the governing field equation and relations. According to Yang (2005), Guz (1999, 2004), Akbarov (2015) and other related references, the equations of the TDLTEWISEPB in the plane strain state in the Ox_1x_2 plane are

$$\frac{\partial \sigma_{11}^{(m)}}{\partial x_1} + \frac{\partial \sigma_{12}^{(m)}}{\partial x_2} + \sigma_{11}^{(m),0} \frac{\partial^2 u_1^{(m)}}{\partial x_1^2} = \rho^{(m)} \frac{\partial^2 u_1^{(m)}}{\partial t^2},$$

$$\frac{\partial \sigma_{12}^{(m)}}{\partial x_1} + \frac{\partial \sigma_{22}^{(m)}}{\partial x_2} + \sigma_{11}^{(m),0} \frac{\partial^2 u_2^{(m)}}{\partial x_1^2} = \rho^{(m)} \frac{\partial^2 u_2^{(m)}}{\partial t^2}, \; m = 1,2,3$$

$$\frac{\partial D_1^{(n)}}{\partial x_1} + \frac{\partial D_2^{(n)}}{\partial x_2} = 0, \; n = 1,3 \tag{2}$$

where $\sigma_{ij}^{(m)}$, $u_i^{(m)}$ and $\rho^{(m)}$ are the components of the stress tensor, components of the displacement vector and mass density of the m-th material, respectively. $D_i^{(n)}$ in the last equation in (2) denotes the electrical displacement of the n-th material. As noted above, we will assume below that the material of the face layers is piezoelectric, but the material of the middle layer is non-linear purely elastic. Consequently, only the first two equations in (2) describe the motion of the core layer of the plate.

Thus, assuming that the piezoelectric material of both the top and bottom face layers is polled along the direction of the Ox_2 axis (with thickness poling), we can write the following constitutive equations for the n-th piezoelectric material in the plane strain state.

$$\sigma_{11}^{(n)} = c_{11}^{(n)} \frac{\partial u_1^{(n)}}{\partial x_1} + c_{13}^{(n)} \frac{\partial u_2^{(n)}}{\partial x_2} + e_{31}^{(n)} \frac{\partial \varphi^{(n)}}{\partial x_2}, \; \sigma_{22}^{(n)} = c_{13}^{(n)} \frac{\partial u_1^{(n)}}{\partial x_1} + c_{33}^{(n)} \frac{\partial u_2^{(n)}}{\partial x_2} + e_{33}^{(n)} \frac{\partial \varphi^{(n)}}{\partial x_2},$$

$$\sigma_{12}^{(n)} = c_{44}^{(n)} \left(\frac{\partial u_1^{(n)}}{\partial x_2} + \frac{\partial u_2^{(n)}}{\partial x_1} \right) + e_{15}^{(n)} \frac{\partial \varphi^{(n)}}{\partial x_1}, \; D_1^{(n)} = e_{15}^{(n)} \left(\frac{\partial u_1^{(n)}}{\partial x_2} + \frac{\partial u_2^{(n)}}{\partial x_1} \right) - \varepsilon_{11}^{(n)} \frac{\partial \varphi^{(n)}}{\partial x_1},$$

$$D_2^{(n)} = e_{31}^{(n)} \frac{\partial u_1^{(n)}}{\partial x_1} + e_{33}^{(n)} \frac{\partial u_2^{(n)}}{\partial x_2} - \varepsilon_{33}^{(n)} \frac{\partial \varphi^{(n)}}{\partial x_2}, \; n = 1,3 \tag{3}$$

where $c_{ij}^{(n)}$ are the elasticity constants, $e_{ij}^{(n)}$ are the piezoelectric constants, $\varepsilon_{ij}^{(n)}$ are the dielectric constants and $D_i^{(n)}$ and $\varphi^{(n)}$ are the components of the electric displacement vector and the electric potential, respectively.

The following linearized elasticity relations are obtained for the middle layer material.

$$\sigma_{11}^{(2)} = A_{11}^{(2)}\varepsilon_{11}^{(2)} + A_{12}^{(2)}\varepsilon_{22}^{(2)},\ \sigma_{22}^{(2)} = A_{12}^{(2)}\varepsilon_{11}^{(2)} + A_{22}^{(2)}\varepsilon_{22}^{(2)},\ \sigma_{12}^{(2)} = 2\mu_{12}^{(2)}\varepsilon_{12}^{(2)} \tag{4}$$

where

$$\varepsilon_{ij}^{(2)} = \frac{1}{2}\left(\frac{\partial u_i^{(2)}}{\partial x_j} + \frac{\partial u_j^{(2)}}{\partial x_i}\right). \tag{5}$$

Linearized relations (4) are obtained and discussed in Appendix A. Moreover, in Appendix A the expressions for the calculation of the coefficients $A_{11}^{(2)}$, $A_{12}^{(2)}$, $A_{22}^{(2)}$, and $\mu_{12}^{(2)}$ of the relation (4) are given through the relation (A5).

Consider the formulation of the contact and boundary conditions. Assume that on the interphase planes $x_2=h_1$ and $x_2=-h_1$, between the piezoelectric face layers and core layer, complete contact conditions for the mechanical displacements and forces are satisfied

$$u_1^{(1)}\Big|_{x_2=h_1} = u_1^{(2)}\Big|_{x_2=h_1},\ u_2^{(1)}\Big|_{x_2=h_1} = u_2^{(2)}\Big|_{x_2=h_1},\ u_1^{(2)}\Big|_{x_2=-h_1} = u_1^{(3)}\Big|_{x_2=-h_1},$$

$$u_2^{(2)}\Big|_{x_2=-h_1} = u_2^{(3)}\Big|_{x_2=-h_1},\ \sigma_{12}^{(1)}\Big|_{x_2=h_1} = \sigma_{12}^{(2)}\Big|_{x_2=h_1},\ \sigma_{22}^{(1)}\Big|_{x_2=h_1} = \sigma_{22}^{(2)}\Big|_{x_2=h_1},$$

$$\sigma_{12}^{(2)}\Big|_{x_2=-h_1} = \sigma_{12}^{(3)}\Big|_{x_2=-h_1},\ \sigma_{22}^{(2)}\Big|_{x_2=-h_1} = \sigma_{22}^{(3)}\Big|_{x_2=-h_1}, \tag{6}$$

where $h_1=H_{core}$.

Moreover, on the interface plane the boundary condition

$$\varphi^{(1)}\Big|_{x_2=h_1} = 0,\ \varphi^{(3)}\Big|_{x_2=-h_1} = 0, \tag{7}$$

for the electric potential or the boundary condition

$$D_2^{(1)}\Big|_{x_2=h_1} = 0,\ D_2^{(3)}\Big|_{x_2=-h_1} = 0, \tag{8}$$

for the electric displacement can be given. On the free face planes of the face layers we write the following conditions

$$\sigma_{12}^{(1)}\Big|_{x_2=h_2} = 0,\ \sigma_{22}^{(1)}\Big|_{x_2=h_2} = 0,\ \sigma_{12}^{(3)}\Big|_{x_2=-h_2} = 0,\ \sigma_{22}^{(3)}\Big|_{x_2=-h_2} = 0, \tag{9}$$

for the mechanical stresses and the boundary condition

$$\varphi^{(1)}\Big|_{x_2=h_2} = 0,\ \varphi^{(3)}\Big|_{x_2=-h_2} = 0, \tag{10}$$

for the electric potential or the boundary condition

$$D_2^{(1)}\Big|_{x_2=h_2}=0\,,\ D_2^{(3)}\Big|_{x_2=-h_2}=0\,, \tag{11}$$

for the electric displacement, where $h_2=H_{core}+H_{PZT}$. Note that the conditions (7) and (10) are called "electrically shorted" or "electroded", but the conditions (8) and (11) are called "electrically open" or "unelectroded".

This completes the consideration of the governing field equations and relations, and formulation of the problem.

3. Method of solution

First we consider the solution procedure of the equations related to the motion of the piezoelectric face layers. As the upper and lower face layers' materials are the same, we therefore, consider the solution procedure only for the upper face piezoelectric layer. Thus, substituting the relations in Eq. (3) into Eq. (2) we obtain the electromechanical-coupled system of equations of motion (equations of electro-elasticity) in terms of the mechanical displacements and electric potential

$$\left(c_{11}^{(1)}+\sigma_{11}^{(1),0}\right)\frac{\partial^2 u_1^{(1)}}{\partial x_1^2}+c_{44}^{(1)}\frac{\partial^2 u_1^{(1)}}{\partial x_2^2}+\left(c_{13}^{(1)}+c_{44}^{(1)}\right)\frac{\partial^2 u^{(1)}}{\partial x_1\partial x_2}+\left(e_{15}^{(1)}+e_{31}^{(1)}\right)\frac{\partial^2\varphi^{(1)}}{\partial x_1\partial x_2}=\rho^{(1)}\frac{\partial^2 u_1^{(1)}}{\partial t^2}\,,$$

$$\left(c_{13}^{(1)}+c_{44}^{(1)}\right)\frac{\partial^2 u_1^{(1)}}{\partial x_1\partial x_2}+\left(c_{44}^{(1)}+\sigma_{11}^{(1),0}\right)\frac{\partial^2 u_2^{(1)}}{\partial x_1^2}+c_{33}^{(1)}\frac{\partial^2 u_2^{(1)}}{\partial x_2^2}+e_{15}^{(1)}\frac{\partial^2\varphi^{(1)}}{\partial x_1^2}+e_{33}^{(1)}\frac{\partial^2\varphi^{(1)}}{\partial x_2^2}=\rho^{(1)}\frac{\partial^2 u_2^{(1)}}{\partial t^2}$$

$$\left(e_{15}^{(1)}+e_{31}^{(1)}\right)\frac{\partial^2 u_1^{(1)}}{\partial x_1\partial x_2}+e_{15}^{(1)}\frac{\partial^2 u_2^{(1)}}{\partial x_1^2}+e_{33}^{(1)}\frac{\partial^2 u_2^{(1)}}{\partial x_2^2}-\varepsilon_{11}^{(1)}\frac{\partial^2\varphi^{(1)}}{\partial x_1^2}-\varepsilon_{33}^{(1)}\frac{\partial^2\varphi^{(1)}}{\partial x_2^2}=0\,. \tag{12}$$

As the harmonic wave propagation in the direction of the Ox_1Ox_1 axis is considered, we can therefore represent the particular solutions for the displacements and electric potential for the face layer as follows

$$u_1^{(1)}=Ae^{bkx_2}\sin(kx_1-\omega t)\,,\ u_2^{(1)}=Be^{bkx_2}\cos\left(kx_1-\omega t\right),\ \varphi^{(1)}=Ce^{bkx_2}\cos(kx_1-\omega t)\,. \tag{13}$$

where A, B and C are unknown constants, k is the wave number, ω is the angular frequency and b is the parameter to be determined.

Substituting the equations (13) into the equations (12) we obtain from the following equations for the unknown constants A, B and C in (13).

$$\left(c_{11}^{(1)}+\sigma_{11}^{(1),0}-c_{44}^{(1)}b^2-\rho^{(1)}\frac{\omega^2}{k^2}\right)A+\left(c_{13}^{(1)}+c_{44}^{(1)}\right)bB+\left(e_{15}^{(1)}+e_{31}^{(1)}\right)bC=0\,,$$

$$\left(c_{13}^{(1)}+c_{44}^{(1)}\right)bA-\left(c_{44}^{(1)}+\sigma_{11}^{(1),0}-c_{33}^{(1)}b^2-\rho^{(1)}\frac{\omega^2}{k^2}\right)B-\left(e_{15}^{(1)}-e_{33}^{(1)}b^2\right)C=0\,,$$

$$\left(e_{15}^{(1)}+e_{31}^{(1)}\right)bA-\left(e_{15}^{(1)}-e_{33}^{(1)}b^2\right)B-\left(\varepsilon_{33}^{(1)}b^2-\varepsilon_{11}^{(1)}\right)C=0\,. \tag{14}$$

In order to get a non-trivial solution for *A*, *B* and *C*, the determinant of the coefficient matrix of Eq. (14) must be zero. Consequently, equating to zero the aforementioned determinant we obtain the equation for determination of the parameter *b*. For a given value of $c=\omega/k$, there are six roots for *b*; each root represents one component of the wave modes propagating in the piezoelectric face layer and yields a partial solution to the piezoelectric face layer. As a result of numerical analyses of the equation with respect to *b* it is established that in the case where $\tilde{c}_2^{(1)}<c<c_1^{(1)}$ the equation has two pure imaginary and four real roots

$$b_1=ip_1,\ b_2=-ip_1,\ b_3=p_2,\ b_4=-p_2,\ b_5=p_3,\ b_6=-p_3, \tag{15}$$

in the case where $c<c_2^{(1)}$ this equation has six real roots

$$b_1=p_1,\ b_2=-p_1,\ b_3=p_2,\ b_4=-p_2,\ b_5=p_3,\ b_6=-p_3, \tag{16}$$

and in the case where $c>c_1^{(1)}$ this equation has four pure imaginary and two real roots

$$b_1=ip_1,\ b_2=-ip_1,\ b_3=ip_2,\ b_4=-ip_2,\ b_5=p_3,\ b_6=-p_3, \tag{17}$$

where

$$\tilde{c}_2^{(1)}=c_2^{(1)}\sqrt{\frac{\sigma_{11}^{(1),0}}{\tilde{c}_{44}^{(1)}}},\ c_2^{(1)}=\sqrt{\frac{\tilde{c}_{44}^{(1)}}{\rho^{(1)}}},\ \tilde{c}_{44}^{(1)}=c_{44}^{(1)}+e_{15}^{(1)}\Big/\varepsilon_{11}^{(1)},$$

$$c_1^{(1)}=\sqrt{\frac{c_{11}^{(1)}}{\rho^{(1)}}},\ i=\sqrt{-1},\ p_1>0,\ p_2>0,\ p_3>0, \tag{18}$$

where the values of p_1, p_2 and p_3 are determined through the numerical solution to the aforementioned equation.

Thus, applying known standard techniques for solution to the system of the ordinary differential equations and doing required mathematical manipulations, we obtain the following expressions for the sought values which appear in the contact (6) and boundary (7)-(11) conditions.

$$u_1^{(1)}=\sum_{i=1}^{6}A_i\varphi_{1i}(x_2)\ ,\ u_2^{(1)}=\sum_{i=1}^{6}A_i\varphi_{2i}(x_2),\ \varphi^{(1)}=\sum_{i=1}^{6}A_i\varphi_{3i}(x_2),$$

$$\sigma_{12}^{(1)}=\sum_{i=1}^{6}A_i\varphi_{12i}(x_2),\ \sigma_{22}^{(1)}=\sum_{i=1}^{6}A_i\varphi_{22i}(x_2),\ D^{(1)}=\sum_{i=1}^{6}A_i\varphi_{4i}(x_2). \tag{19}$$

Note that the expressions of the functions $\varphi_{1i}(x_2)$, $\varphi_{2i}(x_2)$, $\varphi_{3i}(x_2)$, $\varphi_{4i}(x_2)$, $\varphi_{12i}(x_2)$, and $\varphi_{22i}(x_2)$ for each of $c_2^{(1)}<c<c_1^{(1)}$, $c<c_2^{(1)}$, and $c>c_1^{(1)}$ cases are given in Appendix B through the Eqs. (B1), (B2), and (B3), respectively.

Thus, we determine completely the expressions of the sought values related to the piezoelectric face layer and these expressions contain the unknown constants A_1, A_2, ..., A_6 which must be

determined from the foregoing contact and boundary conditions.

As we assume that the geometrical and electro-mechanical properties of the face layers are the same, then by replacing the upper index (1) only in the stresses, displacements, electric displacements and electric potential with the upper index (3) and replacing the unknown constants A_1, A_2, ..., A_6 with unknown constants B_1, B_2, ..., B_6, respectively we obtain the corresponding expressions for the sought values of the lower face piezoelectric layer.

Now we consider the determination of the sought values related to the middle layer. Substituting $\varepsilon_{ij}^{(2)}$ in (5) into the expressions in (4) and substituting the expressions (4) into the equation of motion of the metallic middle layer (i.e., into the first and second equations in (2)) we obtain the following equations of motion in terms of the displacements for the middle layer.

$$\left(A_{11}^{(2)}+\sigma_{11}^{(2),0}\right)\frac{\partial^2 u_1^{(2)}}{\partial x_1^2}+\mu_{12}^{(2)}\frac{\partial^2 u_1^{(2)}}{\partial x_2^2}+\left(A_{12}^{(2)}+\mu_{12}^{(2)}\right)\frac{\partial^2 u_2^{(1)}}{\partial x_1\partial x_2}=\rho^{(2)}\frac{\partial^2 u_1^{(2)}}{\partial t^2},$$

$$\left(A_{12}^{(2)}+\mu_{12}^{(2)}\right)\frac{\partial^2 u_1^{(2)}}{\partial x_1\partial x_2}+\left(\mu_{12}^{(2)}+\sigma_{11}^{(2)0}\right)\frac{\partial^2 u_2^{(2)}}{\partial x_1^2}+A_{22}^{(2)}\frac{\partial^2 u_2^{(2)}}{\partial x_2^2}=\rho^{(2)}\frac{\partial^2 u_2^{(2)}}{\partial t^2}. \tag{20}$$

According to the expressions in (13), we represent the displacements $u_1^{(2)}$ and $u_2^{(2)}$ as follows

$$u_1^{(2)}=\psi_1^{(2)}(x_2)\sin(kx_1-\omega t),\ u_2^{(2)}=\psi_2^{(2)}(x_2)\cos(kx_1-\omega t). \tag{21}$$

Substituting (21) into the Eq. (20) and doing some mathematical manipulations by employing the known solution procedure for a system of ordinary differential equations, we obtain the following expressions for $\psi_1^{(2)}(x_2)$ and $\psi_2^{(2)}(x_2)$

$$\psi_1^{(2)}=Z_1G_1\sinh R_1kx_2+Z_2G_2\cosh R_1kx_2+Z_3G_3\sinh R_2kx_2+Z_4G_4\cosh R_2kx_2,$$

$$\psi_2^{(2)}=Z_1\cosh R_1kx_2+Z_2\sinh R_1kx_2+Z_3\cosh R_2kx_2+Z_4\sinh R_2kx_2, \tag{22}$$

where

$$R_1^{(2)}=\sqrt{-\frac{B_2}{2}+\sqrt{\left(\frac{B_2}{2}\right)^2-C_2}},\ R_2^{(2)}=\sqrt{-\frac{B_2}{2}-\sqrt{\left(\frac{B_2}{2}\right)^2-C_2}},$$

$$B_2=\frac{b_{22}-c_{22}^2}{b_{21}+1},\ C_2=\frac{b_{22}b_{21}}{b_{21}+1},\ G_1=G_2=-\frac{R_1}{c_{22}}-\frac{b_{22}}{c_{22}R_1},\ G_3=G_4=-\frac{R_2}{c_{22}}-\frac{b_{22}}{c_{22}R_2}. \tag{23}$$

In (23) the notation

$$b_{21}=-\frac{1}{\mu_{12}^{(2)}}(A_{11}^{(2)}+\sigma_{11}^{(2)0}),\ c_{21}=\frac{1}{\mu_{12}^{(2)}}(A_{12}^{(2)}+\mu_{12}^{(2)}),$$

$$b_{22}=-\frac{1}{A_{22}^{(2)}}(\mu_{12}^{(2)}+\sigma_{11}^{(2)0}),\ c_{22}=\frac{1}{A_{22}^{(2)}}(A_{12}^{(2)}+\mu_{12}^{(2)}) \tag{24}$$

is used.

Finally, we obtain the following expressions for the displacements and stresses which relate to the middle layer and enter the contact and boundary conditions.

$$u_1^{(2)} = (Z_1 G_1 \sinh R_1 kx_2 + Z_2 G_2 \cosh R_1 kx_2 +$$

$$Z_3 G_3 \sinh R_2 kx_2 + Z_4 G_4 \cosh R_2 kx_2) \sin(kx_1 + \omega t)$$

$$u_2^{(2)} = (Z_1 \cosh R_1 kx_2 + Z_2 \sinh R_1 kx_2 + Z_3 \cosh R_2 kx_2 + Z_4 \sinh R_2 kx_2) \cos(kx_1 + \omega t),$$

$$\sigma_{12}^{(2)} = (Z_1 \mu_{12}^{(2)} (G_1 R_1 - 1) \cosh R_1 kx_2 + Z_2 \mu_{12}^{(2)} (G_2 R_1 - 1) \sinh R_1 kx_2$$

$$+ Z_3 \mu_{12}^{(2)} (G_3 R_2 - 1) \cosh R_2 kx_2 + Z_4 \mu_{12}^{(2)} (G_4 R_2 - 1) \sinh R_2 kx_2) \sin(kx_1 - \omega t),$$

$$\sigma_{22}^{(2)} = (Z_1 (G_1 A_{12}^{(2)} + A_{22}^{(2)} R_1) \sinh R_1 kx_2 + Z_2 (G_2 A_{12}^{(2)} + A_{22}^{(2)} R_1) \cosh R_1 kx_2$$

$$+ Z_3 (G_3 A_{12}^{(2)} + A_{22}^{(2)} R_2) \sinh R_2 kx_2 + Z_4 (G_4 A_{12}^{(2)} + A_{22}^{(2)} R_2) \cosh R_2 kx_2) \cos(kx_1 - \omega t). \qquad (25)$$

It should be noted that the expressions (22) and (25) are obtained for the case where $\operatorname{Im} R_1^{(2)} = \operatorname{Im} R_2^{(2)} = 0$. For other related cases, the corresponding equations can be obtained by employing the well-known solution technique.

This completes consideration of the solution procedures of the equations of motion for the case under consideration.

It is known that, as usual, using the symmetry and asymmetry of the displacements of the sandwich plate, the Lamb waves within are divided into symmetric (extensional) and asymmetric (flexural) ones. In other words, for this division, the condition

$$u_1^{(2)}(x_1, x_2) = u_1^{(2)}(x_1, -x_2) \ , \ u_2^{(2)}(x_1, x_2) = -u_2^{(2)}(x_1, -x_2),$$

$$u_1^{(1)}(x_1, x_2) = u_1^{(3)}(x_1, -x_2) \ , \ u_2^{(1)}(x_1, x_2) = -u_2^{(3)}(x_1, -x_2),$$

$$\varphi^{(1)}(x_1, x_2) = -\varphi^{(3)}(x_1, -x_2). \qquad (26)$$

is used for determination of the extensional (symmetric) Lamb waves and the condition

$$u_1^{(2)}(x_1, x_2) = -u_1^{(2)}(x_1, -x_2) \ , \ u_2^{(2)}(x_1, x_2) = u_2^{(2)}(x_1, -x_2),$$

$$u_1^{(1)}(x_1, x_2) = -u_1^{(3)}(x_1, -x_2) \ , \ u_2^{(1)}(x_1, x_2) = u_2^{(3)}(x_1, -x_2),$$

$$\varphi^{(1)}(x_1, x_2) = \varphi^{(3)}(x_1, -x_2) \qquad (27)$$

is used for determination of the flexural (anti-symmetric) Lamb waves. For acceptability of the conditions (26) and (27), for the subject under consideration, the contact and boundary conditions must be symmetric with respect to the plane x_2=0. According to the relations (6) and (9), the contact and boundary conditions with respect to mechanical forces and displacements are already symmetric with respect to the plane x_2=0. Consequently, for satisfaction of the relations in (26) or (27), it is necessary to assume the symmetry or anti-symmetry of the boundary conditions with respect to the electric potential and electric displacements. In other words, for satisfaction of the

relations (26) and (27) it is also necessary to assume that the same boundary conditions are satisfied on the upper and lower interface planes and the same boundary conditions are satisfied on the free face planes of the lower and upper piezoelectric layers with respect to the electric potential or with respect to the electric displacements.

Thus, taking the condition (26) into account and substituting the expressions (19) and (25) into the contact (6) and boundary conditions (7)-(11), we obtain the system of algebraic equations for the unknown constants $A_1^{(1)}$, $A_2^{(1)}$, …, $A_6^{(1)}$, Z_2 and Z_4. The explicit expressions of these equations are given in Appendix C through the expressions (C1).

For existence of the non-trivial solution of the system of algebraic equations in (C1) the determinant of the coefficients' matrix of this equation must be equal to zero, i.e.

$$\det\left\|\alpha_{nm}(c,kh)\right\| = 0,\ n,m = 1,2,...,8. \tag{28}$$

This equation is the dispersion equation of the extensional waves propagated in the sandwich plate under consideration. The expressions for the coefficients α_{nm} (c,kh) in (28) can be easily determined from the Eq. (C1) in Appendix C and therefore are not given here.

Moreover, taking the conditions in (27) into consideration and doing similar mathematical calculations we obtain the following equations for the flexural Lamb waves, i.e., the equations for the unknowns A_1, A_2, …, A_6, Z_1 and Z_3. The explicit expression of these equations are given in Appendix C through the expressions (C2) and last six equations in (C1).

Thus, according to the aforementioned procedure, we obtain the dispersion equation

$$\det\left\|\beta_{nm}(c,kh)\right\| = 0,\ n,m = 1,2,...,8. \tag{29}$$

The expressions for the components β_{nm} can be easily determined from the equations in (C2) and from the last six equations in (C1).

This completes consideration of the solution method and obtaining the dispersion equations.

4. Numerical results and discussions

We will consider the results related to the dependence between $c/c_2^{(2)}$ and kH (where $c_2^{(2)} = \sqrt{\mu^{(2)}/\rho^{(2)}}$, $H = 2H_{core} + 2H_{PZT}$). These results are obtained by numerical solution of the dispersion Eq. (28) (for the extensional Lamb waves) and (29) (for the flexural Lamb waves).

Note that the numerical solution to the dispersion Eqs. (28) and (29) is carried out by employing the well-known "bi-section" algorithm and corresponding PC programs in MATLAB. Analyses are made for the materials, the mechanical, piezoelectrical and dielectrical properties of which are given in Table 1 and the material of the middle layer is selected as Aluminum (Al) or Steel (St), but the material of the face layer is selected as PZT-2 or PZT-6B. The values of the mechanical constants for the Al and St are taken from the Jin *et al*. (2002), Guz and Makhort (2000) references, respectively, but the values of the mechanical, pizoelectrical and dielectrical constants related to PZT-2 and PZT-6B are taken from the Pang *et al*. (2008) and Yang (2005) references, respectively.

Before beginning the analysis of the dispersion curves we note the following statement. Numerical results show that in the cases where the face planes of the piezoelectric layers are unelectroded (i.e., satisfying the conditions (8) and (11)) the influence of the piezoelectricity of the

Table 1 The values of the mechanical, piezoelectrical and dielectrical properties of the selected materials

Designation	Materials			
	Aluminum	Steel	PZT-2	PZT-6B
$\rho(\times 10^3 kg/m^3)$	2.70	7.795	7.60	7.55
$c_{11}(\times 10^{10} N/m^2)$	10.20	24.76	13.50	16.80
$c_{33}(\times 10^{10} N/m^2)$	10.20	24.76	11.30	16.30
$c_{44}(\times 10^{10} N/m^2)$	2.60	7.75	2.22	3.55
$c_{13}(\times 10^{10} N/m^2)$	5.0	9.26	6.81	8.42
$e_{15}(C/m^2)$	_	_	9.8	4.60
$e_{33}(C/m^2)$	_	_	9	7.10
$e_{31}(C/m^2)$	_	_	-1.9	-0.90
$\varepsilon_{11}(\times 10^{-9} F/m)$	_	_	8.7615	3.60
$\varepsilon_{33}(\times 10^{-9} F/m)$	_	_	3.9825	3.42
$a(\times 10^5 MPa)$	3.08	-2.35	_	_
$b(\times 10^5 MPa)$	-0.49	-2.75	_	_
$c(\times 10^5 MPa)$	-2.92	-4.90	_	_
$\lambda(\times 10^4 MPa)$	5.0	9.26	_	_
$\mu(\times 10^4 MPa)$	2.60	7.75	_	_

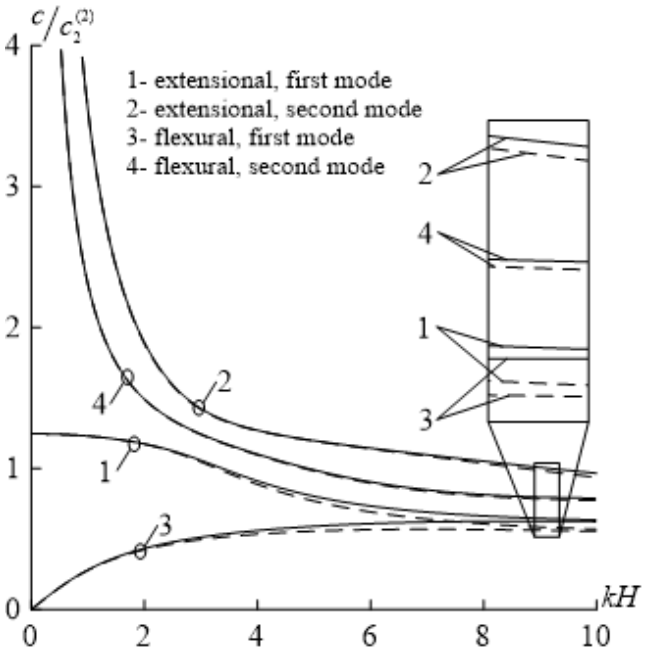

Fig. 2 Dispersion curves of the extensional and flexural Lamb waves in the first two modes for the PZT-2/St/PZT-2 system in the case where H_{PZT}/H_{core}=4. Dashed lines relate to the case where the piezoelectric and dielectric constants of the face layer material are equated to zero

face layer materials on the dispersion curves is insignificant. Therefore, we will consider only the results related to the cases where the face planes of the piezoelectric layers are electroded (i.e., the cases where the conditions (7) and (10) are satisfied) under which the aforementioned influence becomes more considerable.

In all the figures below, the graphs shown by solid lines relate to the cases where the values of the piezoelectric and dielectric constants of the face layers' materials are taken as given in Table 1. However, the graphs shown by dashed lines relate to the cases where the values of the piezoelectric and dielectric constants of the piezoelectric face layers' materials are equated to zero. Consequently, according to the difference between the dashed and solid lines in the figures, which will be given below, certain conclusions can be made as to the effect of the piezoelectricity of the piezoelectric face layers' materials on the influence of the initial stresses on the extensional and flexural Lamb wave propagation velocities.

Thus, we begin consideration and analysis of the numerical results. First, we consider the dispersion curves related to the case where the initial stresses in the constituents of the system are absent, i.e., the case where $\sigma_{11}^{(1),0}=\sigma_{11}^{(2),0}=\sigma_{11}^{(3),0}=0$. These dispersion curves of the extensional and flexural Lamb waves in the first and second modes are given in Figs. 2, 3, 4 and 5 for the PZT-2/St/PZT-2, PZT-2/Al/PZT-2, PZT-6B/St/PZT-6B and PZT-6B/Al/PZT-6B sandwich plates, respectively in the case where H_{PZT}/H_{core}=4. In these figures, the numbers 1 and 2 indicate the dispersion curves of the extensional Lamb waves in the first and second modes, and the numbers 3 and 4 indicate the dispersion curves of the flexural Lamb waves also in the first and second modes, respectively.

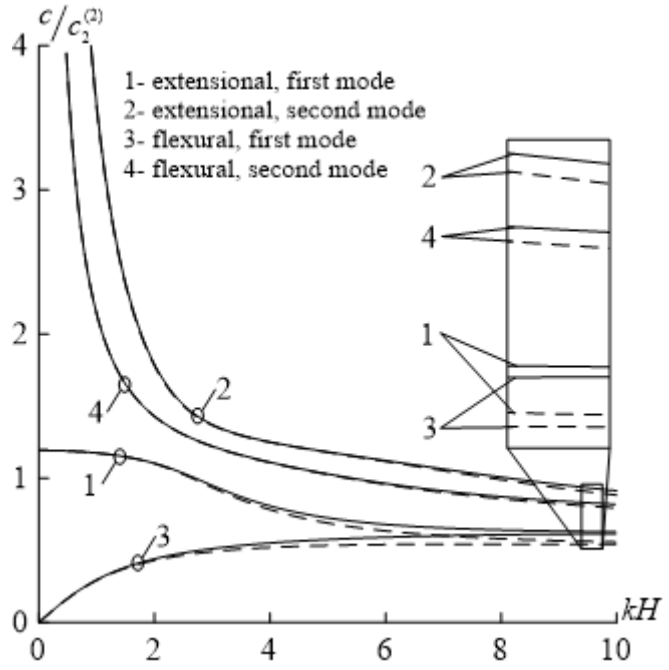

Fig. 3 Dispersion curves of the extensional and flexural Lamb waves in the first two modes for the PZT-2/Al/PZT-2 system in the case where H_{PZT}/H_{core}=4. Dashed lines relate to the case where the piezoelectric and dielectric constants of the face layer material are equated to zero

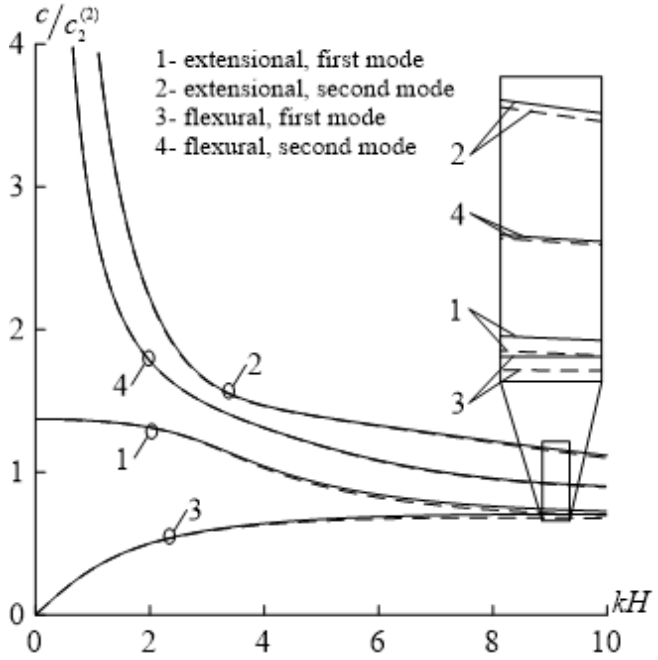

Fig. 4 Dispersion curves of the extensional and flexural Lamb waves in the first two modes for the PZT-6B/St/PZT-6B system in the case where H_{PZT}/H_{core}=4. Dashed lines relate to the case where the piezoelectric and dielectric constants of the face layer material are equated to zero

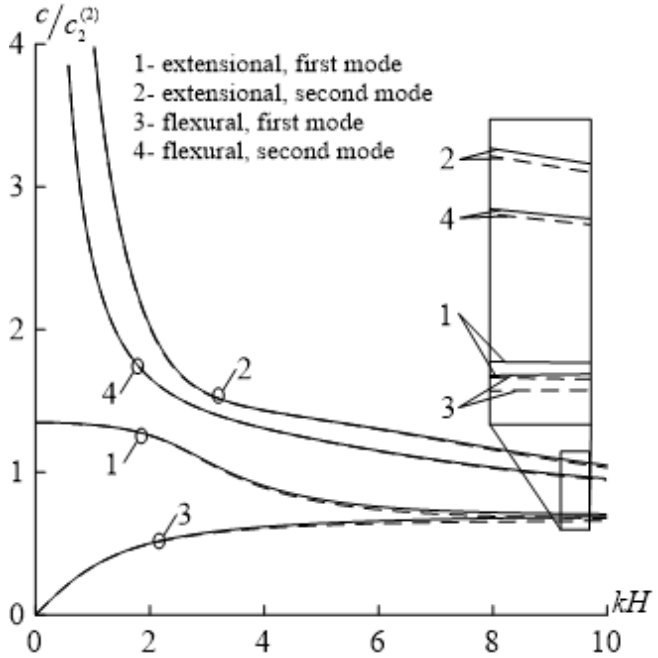

Fig. 5 Dispersion curves of the extensional and flexural Lamb waves in the first two modes for the PZT-6B/Al/PZT-6B system in the case where H_{PZT}/H_{core}=4. Dashed lines relate to the case where the piezoelectric and dielectric constants of the face layer material are equated to zero

It follows from Figs. 2-5 that the piezoelectricity of the face layers' material causes the extensional and flexural Lamb wave propagation velocity in each mode and for all considered sandwich plate materials, to increase. The magnitude of the increase in the wave propagation velocity caused by the effect of the piezoelectricity of the face layers' materials grows with *kH* for both modes and this increase is explained by the "stiffening" effects of the piezoelectric materials. Moreover, the results given in Figs. 2-5 show that the dispersion curves given in these figures are similar (in the qualitative sense) with the corresponding ones obtained in the papers by Akbarov *et al*. (2008, 2011) and detailed in the monograph by Akbarov (2015) for the sandwich plates with layers made of purely elastic materials. Consequently, this similarity guarantees the reliability of the calculation algorithm and PC programs used.

As noted above, the main objective of the numerical investigations in the present paper is the study and analysis of the influence of the initial stresses on the wave propagation velocity. Thus, we begin this analysis and in order to estimate the magnitude of the influence, we introduce the parameters

$$\psi^{(1)}=\frac{\sigma_{11}^{(1),0}}{c_{44}^{(1)}}\ ,\ \psi^{(2)}=\frac{\sigma_{11}^{(2),0}}{\mu^{(2)}}\ ,\ \psi^{(3)}=\frac{\sigma_{11}^{(3),0}}{c_{44}^{(1)}}\ ,\ \eta=10^3\times(\overline{c}-c)/c_2^{(2)}, \tag{30}$$

where c is the wave propagation velocity in the case where the initial stresses are absent in the constituents of the system under consideration and $\overline{c}$ is the wave propagation velocity in the case where the initial stresses exist in both the face layers or in the core layer of the sandwich plate.

Below we will consider the graphs of the dependence between the parameter η and kH constructed for various values of the parameters $\psi^{(1)}=\psi^{(3)}$ and $\psi^{(2)}$, and for various sets of materials for the extensional and flexural Lamb waves in the first and second modes, and given in Figs. 6-27. Moreover, in Figs. 6-27, the graphs grouped by letters *a*, *b*, *c* and *d* relate to the cases where H_{PZT}/H_{core}=0.5, H_{PZT}/H_{core}=1, H_{PZT}/H_{core}=2 and H_{PZT}/H_{core}=4, respectively. In the considered cases, it is assumed that the layers of the plate are stressed initially and are then connected with each other.

Also, in the graphs grouped by the letters a, b and c, the range of change of the dimensionless wavenumber kH is (0,10]. However, in the graphs grouped by the letter d, in order to illustrate the high wavenumber asymptotic values of the parameter η, besides the range of change of kH, parts of the graphs in the near vicinity of kH=60 are also added.

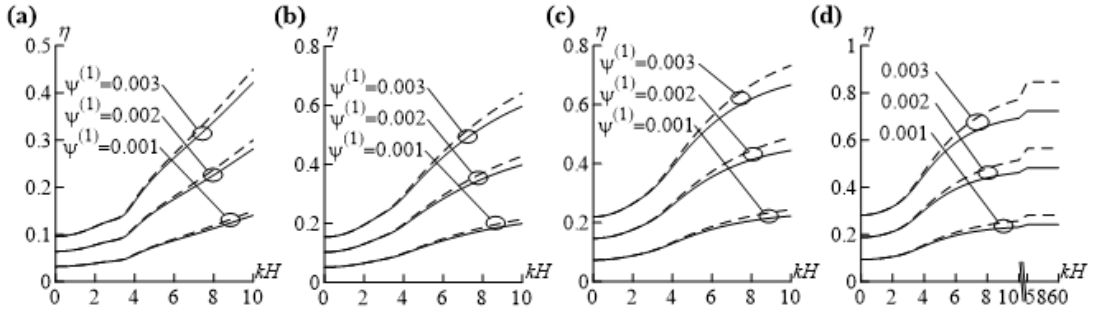

Fig. 6 The influence of the parameter $\psi^{(1)}=\psi^{(3)}$ (>0) on the extensional Lamb wave propagation velocity in the first mode for the PZT-2/St/PZT-2 system in the case where $\psi^{(2)}$=0 and H_{PZT}/H_{core}=0.5 (a); H_{PZT}/H_{core}=1 (b); H_{PZT}/H_{core}=2 (c); H_{PZT}/H_{core}=4 (d)

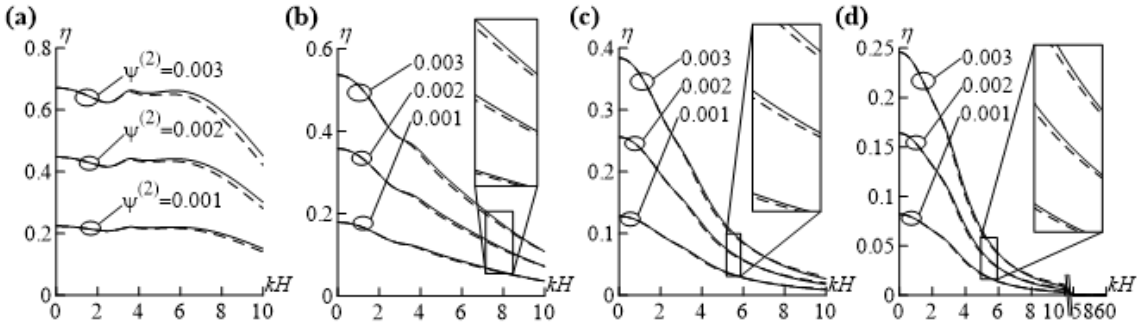

Fig. 7 The influence of the parameter $\psi^{(2)}$ (>0) on the extensional Lamb wave propagation velocity in the first mode for the PZT-2/St/PZT-2 system in the case where $\psi^{(1)}=0$, $a^{(2)}=b^{(2)}=c^{(2)}=0$ and $H_{PZT}/H_{core}=0.5$ (a); $H_{PZT}/H_{core}=1$ (b); $H_{PZT}/H_{core}=2$ (c); $H_{PZT}/H_{core}=4$ (d)

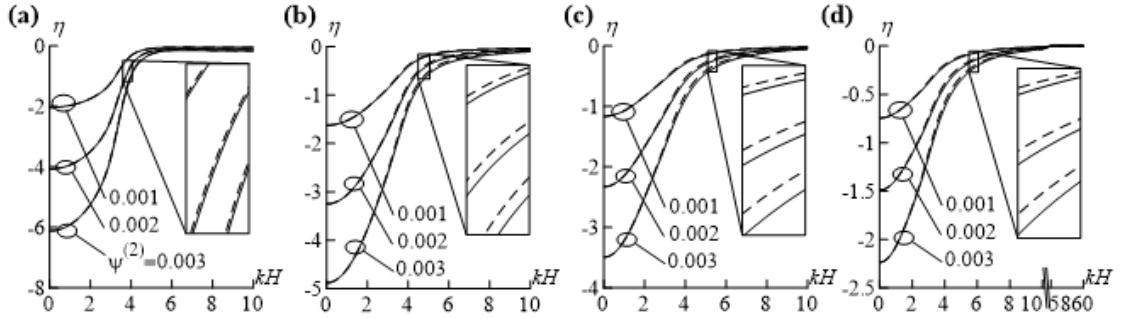

Fig. 8 The influence of the parameter $\psi^{(2)}$ (>0) on the extensional Lamb wave propagation velocity in the first mode for the PZT-2/St/PZT-2 system in the case where $\psi^{(1)}=0$, $a^{(2)}\neq0$, $b^{(2)}\neq0$, $c^{(2)}\neq0$ and $H_{PZT}/H_{core}=0.5$ (a); $H_{PZT}/H_{core}=1$ (b); $H_{PZT}/H_{core}=2$ (c); $H_{PZT}/H_{core}=4$ (d)

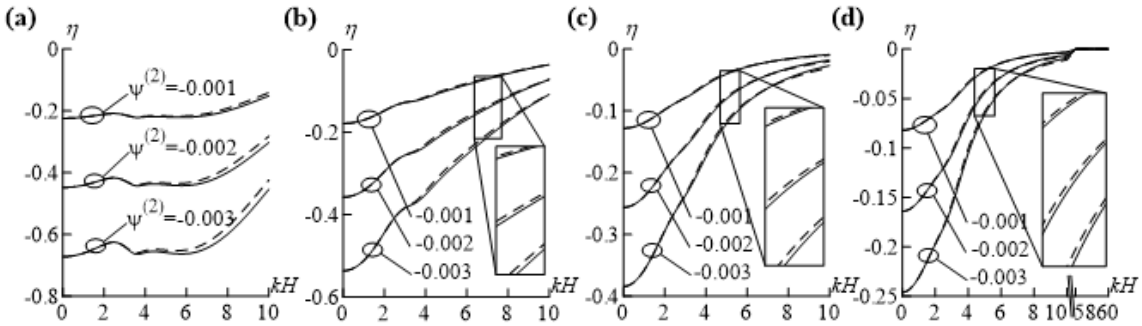

Fig. 9 The influence of the parameter $\psi^{(2)}$ (<0) on the extensional Lamb wave propagation velocity in the first mode for the PZT-2/St/PZT-2 system in the case where $\psi^{(1)}=0$, $a^{(2)}=b^{(2)}=c^{(2)}=0$ and $H_{PZT}/H_{core}=0.5$ (a); $H_{PZT}/H_{core}=1$ (b); $H_{PZT}/H_{core}=2$ (c); $H_{PZT}/H_{core}=4$ (d)

First we consider the results related to the dependencies between η and kH, and obtained for the sandwich plate PZT-2/St/PZT-2. These results for the first mode of the extensional (flexural) waves are given in Figs. 6-10 (in Figs. 11-15). Under construction of the graphs given in Figs. 6 and 11 it is assumed that $\psi^{(1)}$ ($=\psi^{(3)}$)>0 and $\psi^{(2)}=0$. Moreover, under construction of the graphs

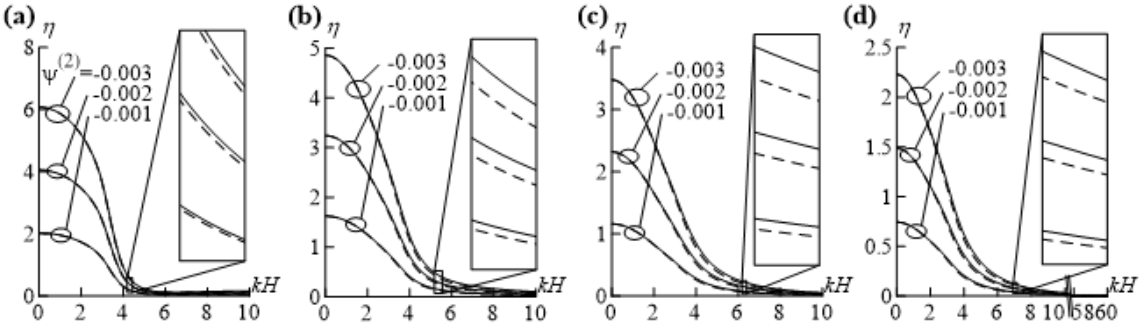

Fig. 10 The influence of the parameter $\psi^{(2)}$ (<0) on the extensional Lamb wave propagation velocity in the first mode for the PZT-2/St/PZT-2 system in the case where $\psi^{(1)}=0$, $a^{(2)}\neq 0$, $b^{(2)}\neq 0$, $c^{(2)}\neq 0$ and $H_{PZT}/H_{core}=0.5$ (a); $H_{PZT}/H_{core}=1$ (b); $H_{PZT}/H_{core}=2$ (c); $H_{PZT}/H_{core}=4$ (d)

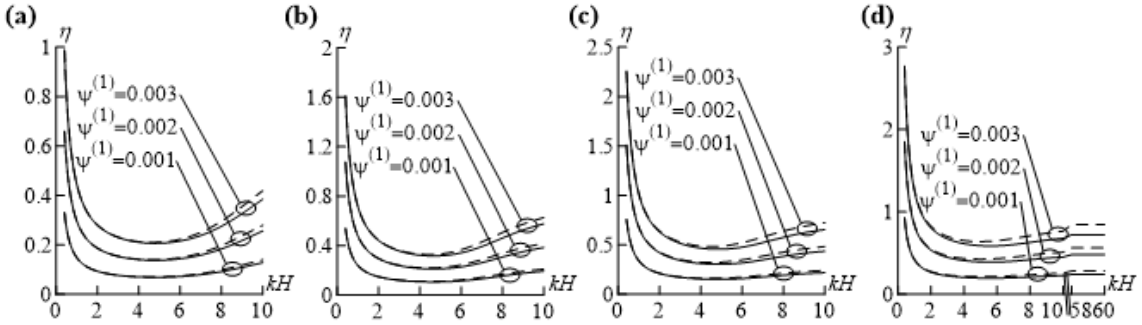

Fig. 11 The influence of the parameter $\psi^{(1)}=\psi^{(3)}$ (>0) on the flexural Lamb wave propagation velocity in the first mode for the PZT-2/St/PZT-2 system in the case where $\psi^{(2)}=0$ and $H_{PZT}/H_{core}=0.5$ (a); $H_{PZT}/H_{core}=1$ (b); $H_{PZT}/H_{core}=2$ (c); $H_{PZT}/H_{core}=4$ (d)

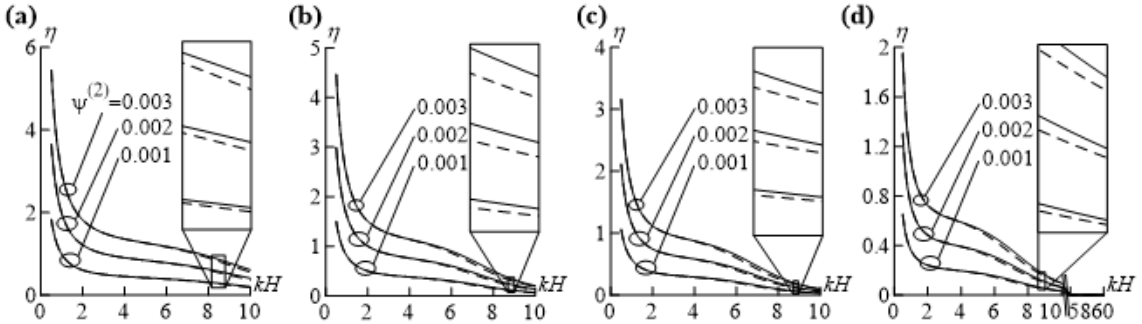

Fig. 12 The influence of the parameter $\psi^{(2)}$ (>0) on the flexural Lamb wave propagation velocity in the first mode for the PZT-2/St/PZT-2 system in the case where $\psi^{(1)}=0$, $a^{(2)}=b^{(2)}=c^{(2)}=0$ and $H_{PZT}/H_{core}=0.5$ (a); $H_{PZT}/H_{core}=1$ (b); $H_{PZT}/H_{core}=2$ (c); $H_{PZT}/H_{core}=4$ (d)

given in Figs. 7 and 12 (in Figs. 9 and 14) it is assumed that $\psi^{(1)}$ (=$\psi^{(3)}$)=0, $\psi^{(2)}>0$ ($\psi^{(2)}<0$) and $a^{(2)}=b^{(2)}=c^{(2)}=0$, i.e., the influence of the third order elastic constants which enter into the relations in (9) of the core layer material on the considered dependencies is not taken into consideration. Note that the graphs illustrated in Figs. 8 and 13 (Figs. 10 and 15) are also obtained in the cases

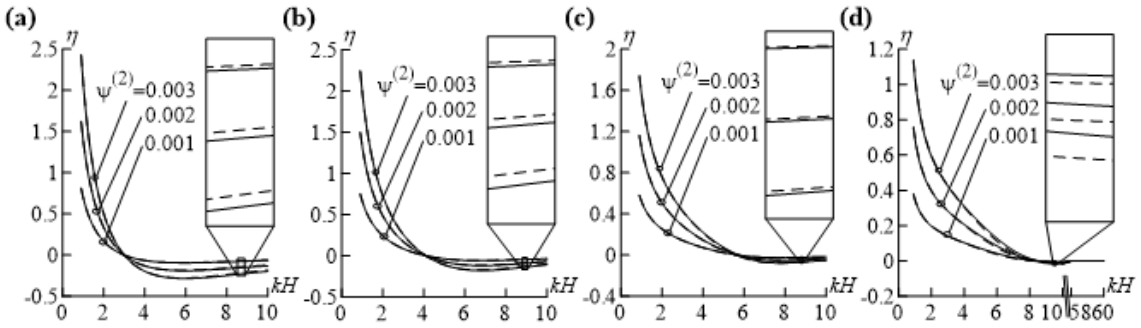

Fig. 13 The influence of the parameter $\psi^{(2)}$ (>0) on the flexural Lamb wave propagation velocity in the first mode for the PZT-2/St/PZT-2 system in the case where $\psi^{(1)}=0$, $a^{(2)}\neq 0$, $b^{(2)}\neq 0$, $c^{(2)}\neq 0$ and $H_{PZT}/H_{core}=0.5$ (a); $H_{PZT}/H_{core}=1$ (b); $H_{PZT}/H_{core}=2$ (c); $H_{PZT}/H_{core}=4$ (d)

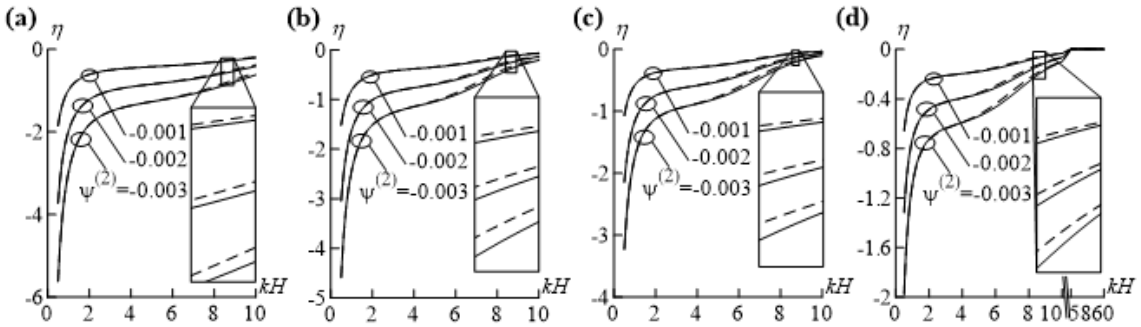

Fig. 14 The influence of the parameter $\psi^{(2)}$ (<0) on the flexural Lamb wave propagation velocity in the first mode for the PZT-2/St/PZT-2 system in the case where $\psi^{(1)}=0$, $a^{(2)}=b^{(2)}=c^{(2)}=0$ and $H_{PZT}/H_{core}=0.5$ (a); $H_{PZT}/H_{core}=1$ (b); $H_{PZT}/H_{core}=2$ (c); $H_{PZT}/H_{core}=4$ (d)

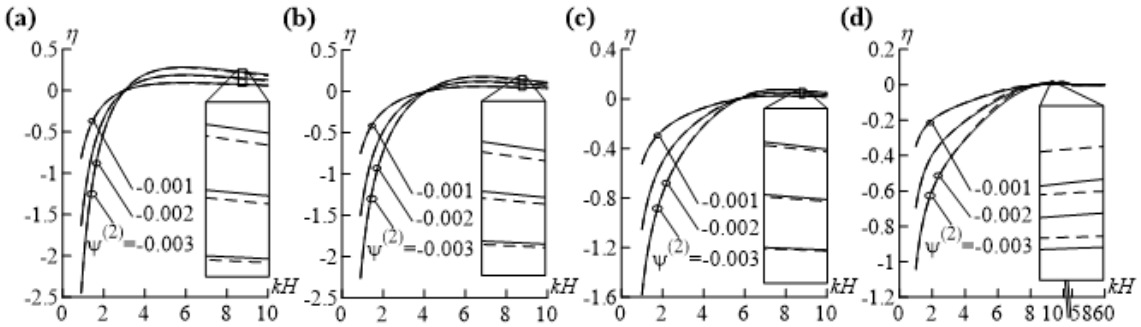

Fig. 15 The influence of the parameter $\psi^{(2)}$ (<0) on the flexural Lamb wave propagation velocity in the first mode for the PZT-2/St/PZT-2 system in the case where $\psi^{(1)}=0$, $a^{(2)}\neq 0$, $b^{(2)}\neq 0$, $c^{(2)}\neq 0$ and $H_{PZT}/H_{core}=0.5$ (a); $H_{PZT}/H_{core}=1$ (b); $H_{PZT}/H_{core}=2$ (c); $H_{PZT}/H_{core}=4$ (d)

considered in Figs. 7 and 12 (Figs. 9 and 14), respectively, however, under construction of these graphs, the influence of the third order elastic constants on the investigated dependencies is taken into consideration, i.e., it is assumed that $a^{(2)}\neq 0$, $b^{(2)}\neq 0$, and $c^{(2)}\neq 0$.

Thus, it follows from Figs. 6 and 11 that pre-stretching of the piezoelectric face layers causes

an increase in the values of the extensional and flexural Lamb waves' propagation velocity. The magnitude of this increase grows with H_{PZT}/H_{core} and with $\psi^{(1)}$, i.e., with the piezoelectric face layers' thickness and with the initial stretching of this layer. Moreover, it follows from these figures that as a result of the piezoelectricity of the face layers' material the influence of the initial stresses, i.e., the influence of the parameter $\psi^{(1)}$ on the wave propagation velocity decreases and the magnitude of this decrease grows with kH and approaches the high wavenumber limit value of η as $kH\rightarrow\infty$ (see Figs. 6(d) and 11(d)). The results also show that the wave propagation velocity (or the values of the parameter η) for the extensional Lamb waves increases monotonically with kH. However, dependence between the parameter η and kH obtained for the flexural Lamb waves is non-monotonic. At the same time, as observed from the graphs, the influence of the initial stretching of the face piezoelectric layers on the wave propagation velocity also depends significantly on the values of the dimensionless wavenumber kH.

Now, we attempt to explain the foregoing results using the corresponding physico-mechanical considerations. This explanation is based on the fact that an increase (a decrease) in the stiffness of the elastic or PZT+elastic systems for the constant material density causes an increase (a decrease) in the values of the wave propagation velocity. In the foregoing results, it is considered that the face PZT layers of the sandwich plate under consideration are initially stretched. As a result of this initial stretching, the stiffness of the sandwich plate increases, which causes an increase in the Lamb wave propagation velocity.

It is evident that the piezoelectricity of the face layers absorbs a certain part of the mechanical work done by the initial stresses, consequently, the piezoelectricity of the face layers causes a decrease in the stiffness grow of the sandwich plate, which appears as a result of the mentioned initial stretching. Namely with this, it can be explained that the influence of the initial stretching on the Lamb wave propagation velocity obtained in the case where the piezoelectricity of the face layers is ignored, is more considerable than that obtained in the case where the piezoelectricity of these layers is taken into consideration.

Finally, we note that the explanation of the difference of the character of the dependencies between the parameter η and kH obtained for the extensional and flexural Lamb waves can be made with the difference of the modes of these waves.

It should be noted that in the case where the constitutive relations of the constituents are linear, the explanation mechanism given above can be used to explain all the corresponding numerical results obtained in the present paper. However, in the case where the initial stretching (the initial compression) is applied to the constituents of the sandwich plate with the linearized constitutive relations obtained from the linearization of the corresponding non-linear constitutive relation, for instance from the linearization of the non-linear constitutive relations based on the Murnaghan potential, this initial stretching (initial compression) may cause a decrease (an increase) in the stiffness of the plate, which may cause a decrease (an increase) in the wave propagation velocity. This fact must be taken into consideration to understand the difference between the results, for instance, given in Figs. 7 and 8, i.e., to understand the influence of the third order elastic constants of the core layer material on the Lamb wave propagation velocity in the sandwich plate under consideration.

We recall that the graphs illustrated in Figs. 7 and 12 (in Figs. 9 and 14) are constructed in the case where $\psi^{(2)}>0$ ($\psi^{(2)}<0$) under $a^{(2)}=b^{(2)}=c^{(2)}=0$ and also recall that the graphs illustrated in Figs. 7 and 9 (in Figs. 12 and 14) relate to the extensional (flexural) waves. Thus, it follows from the results that the initial stretching (compression) of the core metal layer of the plate in the case where $a^{(2)}=b^{(2)}=c^{(2)}=0$ causes an increase (a decrease) in the values of the wave propagation

velocity. However, the magnitude of this decrease in the case where $\psi^{(2)}<0$ is more significant than the magnitude of the increase in the case where $\psi^{(2)}>0$. Moreover, the results show that the magnitude of the influence of the initial stresses on the wave propagation velocity decreases with H_{PZT}/H_{core} and increases with the absolute values of $\psi^{(2)}$. The influence of the piezoelectricity of the face layers' materials on the wave propagation velocity is insignificant and causes an increase in the values of this velocity. According to Figs. 7 and 12, as well as Figs. 9 and 14, in the case where $\psi^{(2)}>0$ ($\psi^{(2)}<0$) the influence of the initial stretching (compression) on the wave propagation velocity decreases with the dimensionless wavenumber kH.

Analyze the results given in Figs. 8 and 13 (in Figs. 10 and 15) which show the results obtained in the cases where $\psi^{(2)}>0$ ($\psi^{(2)}<0$) under $a^{(2)}\neq 0$, $b^{(2)}\neq 0$ and $c^{(2)}\neq 0$. Comparison of these results with the corresponding ones given in Figs. 7 and 12 (in Figs. 9 and 14) allows us to conclude that in taking the third order elastic constants of the metal elastic core layer into consideration significantly affects the influence of the initial stresses in this layer on the wave propagation velocity. It should be noted that this effect has not only a quantitative, but also a qualitative character. It follows from Fig. 8 that in contrast to the case considered in Fig. 7, the initial stretching of the core layer causes a decrease in the values of the extensional Lamb wave propagation velocity. The magnitude of this decrease grows with $\psi^{(2)}$ and decreases with H_{PZT}/H_{core}. Moreover, it follows from Fig. 13 that in contrast to the case considered in Fig. 12, the character of the influence of the initial stretching of the middle layer on the flexural wave propagation velocity depends on the dimensionless wavenumber kH. So, there exists such a value of kH (denote it by $(kH)'$) before which (after which), i.e., in the cases where $kH<(kH)'$ ($kH>(kH)'$) as a result of the initial stretching of the core layer, the wave propagation velocity increases (decreases). Consequently, in the case where $kH=(kH)'$ the initial stretching of the core layer does not act on the wave propagation velocity.

Comparison of the results given in Fig. 15 shows that as a result of taking the third order elastic constants into consideration the character of the influence of the initial compression on the flexural wave propagation velocity also depends on the dimensionless wavenumber kH. So, there exists such a value of kH (denote it by $(kH)''$) before which (after which), i.e., in the cases where $kH<(kH)''$ ($kH>(kH)''$), as a result of the initial compression of the core layer, the wave propagation velocity decreases (increases). Consequently, in the case where $kH=(kH)''$ the initial compression of the core layer does not act on the wave propagation velocity. The results also show that $(kH)'\approx(kH)''$.

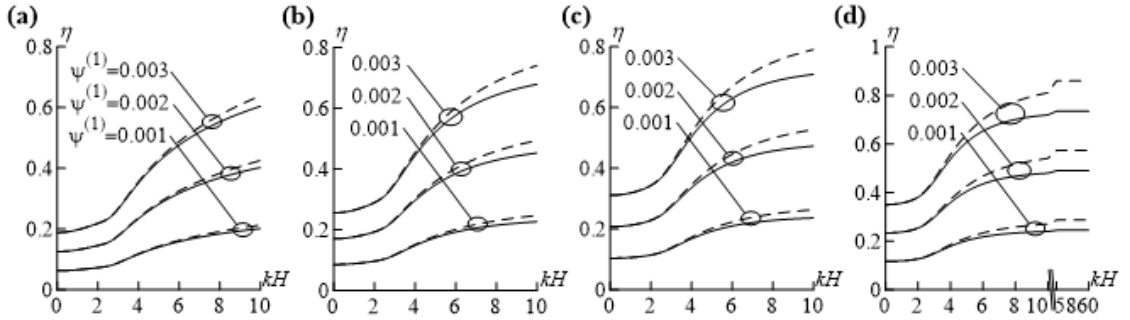

Fig. 16 The influence of the parameter $\psi^{(1)}=\psi^{(3)}$ (>0) on the extensional Lamb wave propagation velocity in the first mode for the PZT-2/Al/PZT-2 system in the case where $\psi^{(2)}=0$ and $H_{PZT}/H_{core}=0.5$ (a); $H_{PZT}/H_{core}=1$ (b); $H_{PZT}/H_{core}=2$ (c); $H_{PZT}/H_{core}=4$ (d)

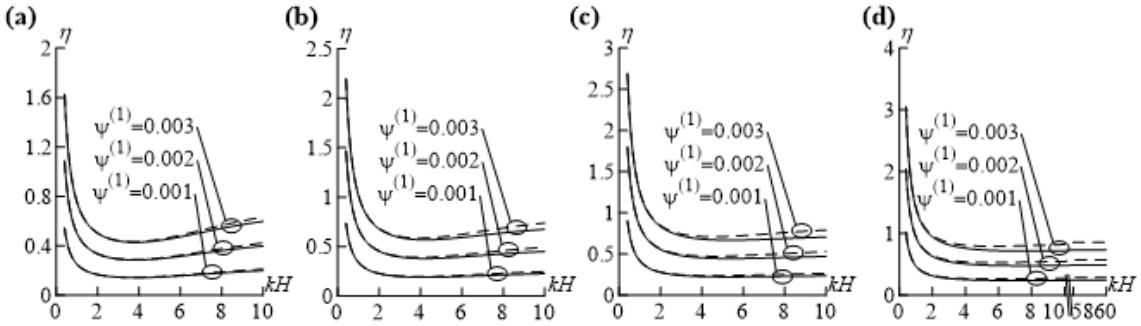

Fig. 17 The influence of the parameter $\psi^{(1)}=\psi^{(3)}$ (>0) on the flexural Lamb wave propagation velocity in the first mode for the PZT-2/Al/PZT-2 system in the case where $\psi^{(2)}=0$ and $H_{PZT}/H_{core}=0.5$ (a); $H_{PZT}/H_{core}=1$ (b); $H_{PZT}/H_{core}=2$ (c); $H_{PZT}/H_{core}=4$ (d)

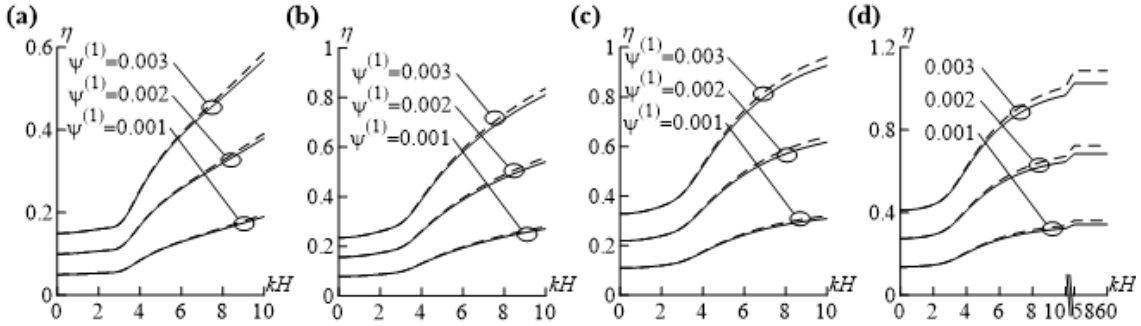

Fig. 18 The influence of the parameter $\psi^{(1)}=\psi^{(3)}$ (>0) on the extensional Lamb wave propagation velocity in the first mode for the PZT-6B/St/PZT-6B system in the case where $\psi^{(2)}=0$ and $H_{PZT}/H_{core}=0.5$ (a); $H_{PZT}/H_{core}=1$ (b); $H_{PZT}/H_{core}=2$ (c); $H_{PZT}/H_{core}=4$ (d)

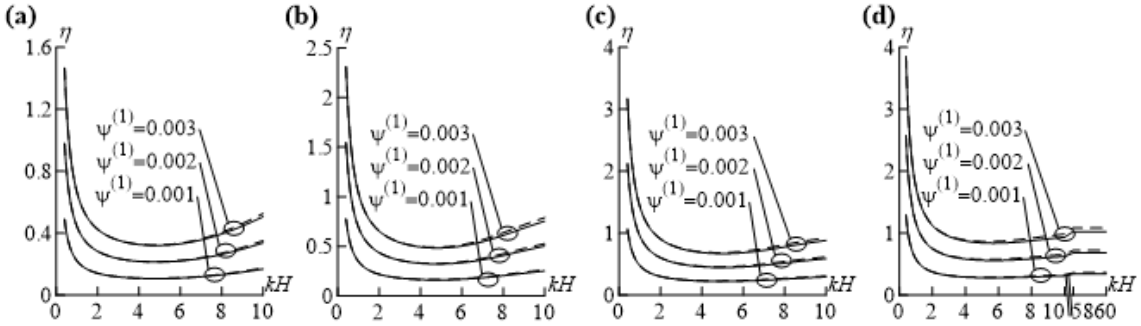

Fig. 19 The influence of the parameter $\psi^{(1)}=\psi^{(3)}$ (>0) on the flexural Lamb wave propagation velocity in the first mode for the PZT-6B/Al/PZT-6B system in the case where $\psi^{(2)}=0$ and $H_{PZT}/H_{core}=0.5$ (a); $H_{PZT}/H_{core}=1$ (b); $H_{PZT}/H_{core}=2$ (c); $H_{PZT}/H_{core}=4$ (d)

Note that similar results are also obtained for the sandwich plate PZT-2 /Al/ PZT-2. The graphs given in Figs. 16 (for the extensional waves) and 17 (for the flexural waves) are examples of these results which relate to the first mode. Moreover, the results obtained for the plates PZT-6B /St/ PZT-6B and PZT-6B /Al/ PZT-6B are, in the qualitative sense, also similar to the foregoing ones.

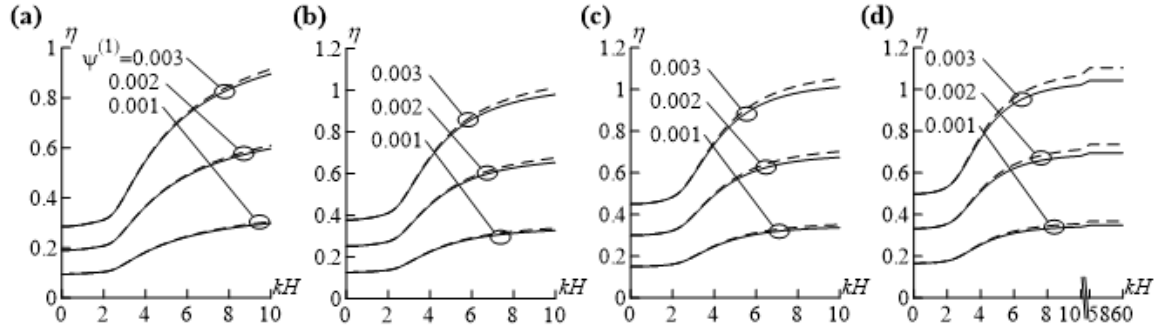

Fig. 20 The influence of the parameter $\psi^{(1)}=\psi^{(3)}$ (>0) on the extensional Lamb wave propagation velocity in the first mode for the PZT-6B/Al/PZT-6B system in the case where $\psi^{(2)}=0$ and $H_{PZT}/H_{core}=0.5$ (a); $H_{PZT}/H_{core}=1$ (b); $H_{PZT}/H_{core}=2$ (c); $H_{PZT}/H_{core}=4$ (d)

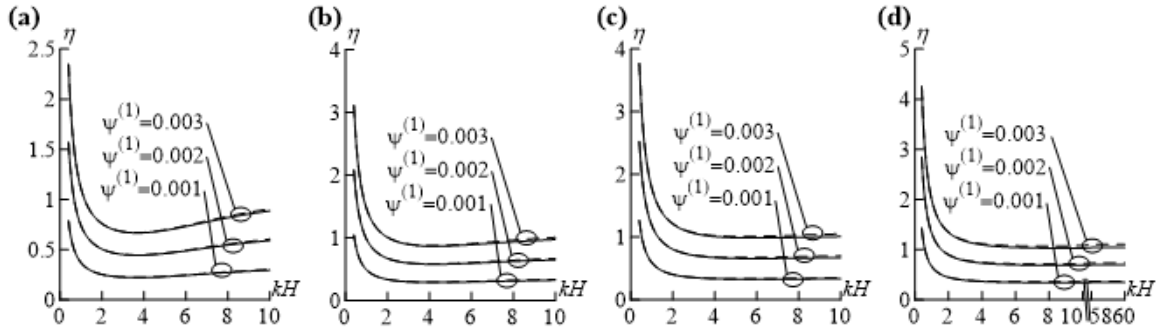

Fig. 21 The influence of the parameter $\psi^{(1)}=\psi^{(3)}$ (>0) on the flexural Lamb wave propagation velocity in the first mode for the PZT-6B/Al/PZT-6B system in the case where $\psi^{(2)}=0$ and $H_{PZT}/H_{core}=0.5$ (a); $H_{PZT}/H_{core}=1$ (b); $H_{PZT}/H_{core}=2$ (c); $H_{PZT}/H_{core}=4$ (d)

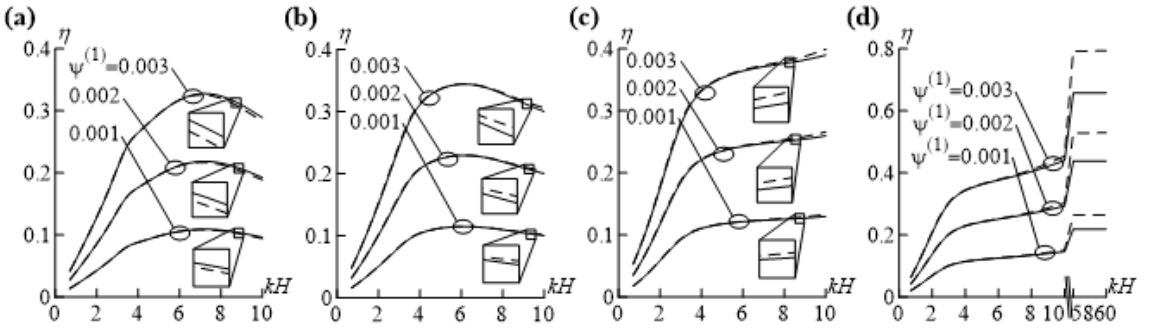

Fig. 22 The influence of the parameter $\psi^{(1)}=\psi^{(3)}$ (>0) on the extensional Lamb wave propagation velocity in the second mode for the PZT-2/St/PZT-2 system in the case where $\psi^{(2)}=0$ and $H_{PZT}/H_{core}=0.5$ (a); $H_{PZT}/H_{core}=1$ (b); $H_{PZT}/H_{core}=2$ (c); $H_{PZT}/H_{core}=4$ (d)

The graphs given in Figs. 18 (extensional waves) and 19 (flexural waves) are examples obtained in the first mode for the plate PZT-6B /St/ PZT-6B, and the graphs given in Figs. 20 (extensional waves) and 21 (flexural waves) are examples also obtained in the first mode for the PZT-6B /Al/ PZT-6B plate. Comparison of the results illustrated in Figs. 18, 19, 20 and 21 with the corresponding

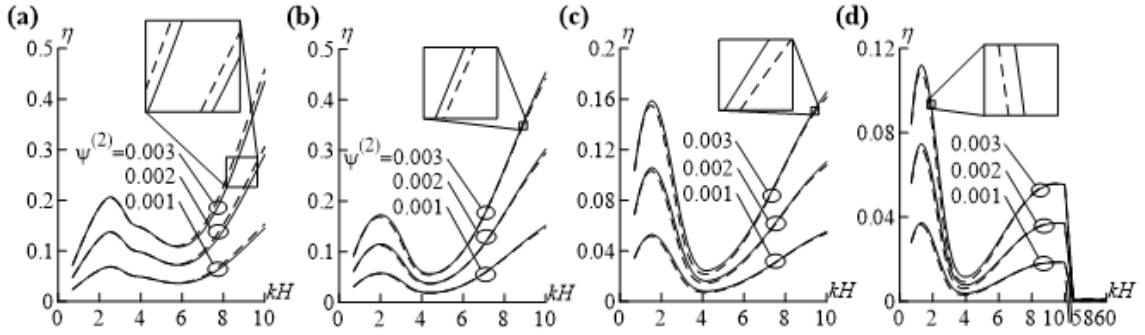

Fig. 23 The influence of the parameter $\psi^{(2)}$ (>0) on the extensional Lamb wave propagation velocity in the second mode for the PZT-2/St/PZT-2 system in the case where $\psi^{(1)}=0$, $a^{(2)}=b^{(2)}=c^{(2)}=0$ and $H_{PZT}/H_{core}=0.5$ (a); $H_{PZT}/H_{core}=1$ (b); $H_{PZT}/H_{core}=2$ (c); $H_{PZT}/H_{core}=4$ (d)

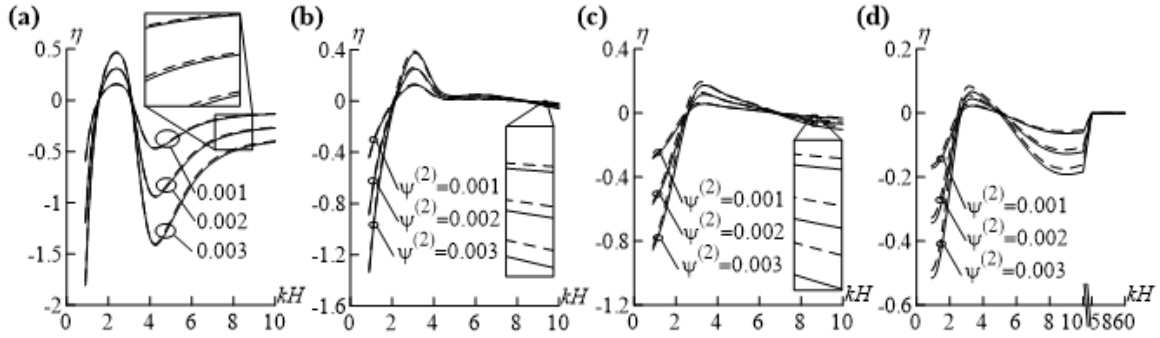

Fig. 24 The influence of the parameter $\psi^{(2)}$ (>0) on the extensional Lamb wave propagation velocity in the second mode for the PZT-2/St/PZT-2 system in the case where $\psi^{(1)}=0$, $a^{(2)}=b^{(2)}=c^{(2)}=0$ and $H_{PZT}/H_{core}=0.5$ (a); $H_{PZT}/H_{core}=1$ (b); $H_{PZT}/H_{core}=2$ (c); $H_{PZT}/H_{core}=4$ (d)

ones given in Figs. 6, 11, 16 and 17 shows that the effect of the piezoelectricity of PZT-2 on the influence of the initial stresses on the wave propagation velocity is more significant than that of PZT-6B.

Taking the last conclusion into consideration we analyze here the graphs of the dependencies between the parameters η and kH in the second mode obtained for the sandwich plate PZT-2 /Al/ PZT-2. Graphs of these dependencies obtained in the case where $\psi^{(1)}$ ($=\psi^{(3)}$)>0 and $\psi^{(2)}=0$ are given in Figs. 22 and 25 for the extensional and flexural waves, respectively. Moreover, the graphs of the studied dependencies obtained in the case where $\psi^{(2)}>0$ and $\psi^{(1)}$ ($=\psi^{(3)}$)=0 under $a^{(2)}=b^{(2)}=c^{(2)}=0$ are given in Figs. 23 and 26, but the graphs obtained under $a^{(2)}\neq 0$, $b^{(2)}\neq 0$ and $c^{(2)}\neq 0$ are given in Figs. 24 and 27, also for the extensional and flexural waves, respectively.

Thus, it follows from the Figs. 22 and 25 that the initial stretching of the piezoelectric face layers of the plate causes the wave propagation velocity in the second mode to increase. The character of the influence of the piezoelectricity of the face layers' materials depends on the values of kH, so there exists such a value of kH (denote it by $(kH)^*$) before which (after which) the piezoelectricity causes a decrease (an increase) in the values of the parameter η and the magnitude of this increase grows with kH under $kH>(kH)^*$.

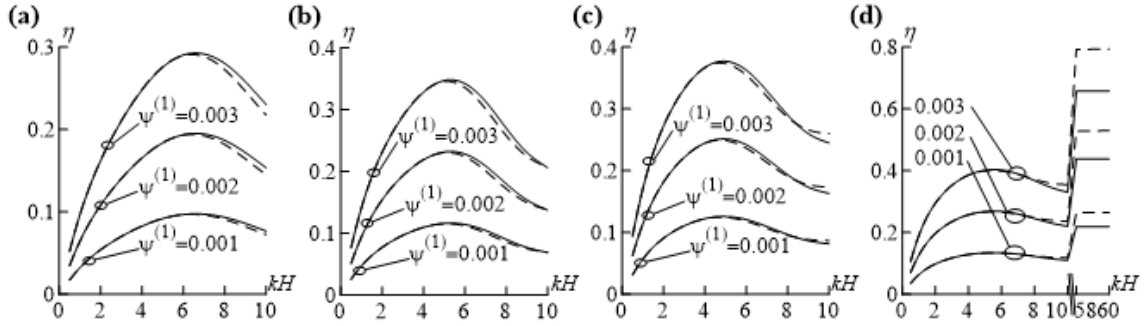

Fig. 25 The influence of the parameter $\psi^{(1)}=\psi^{(3)}$ (>0) on the flexural Lamb wave propagation velocity in the second mode for the PZT-2/St/PZT-2 system in the case where $\psi^{(2)}=0$ and $H_{PZT}/H_{core}=0.5$ (a); $H_{PZT}/H_{core}=1$ (b); $H_{PZT}/H_{core}=2$ (c); $H_{PZT}/H_{core}=4$ (d)

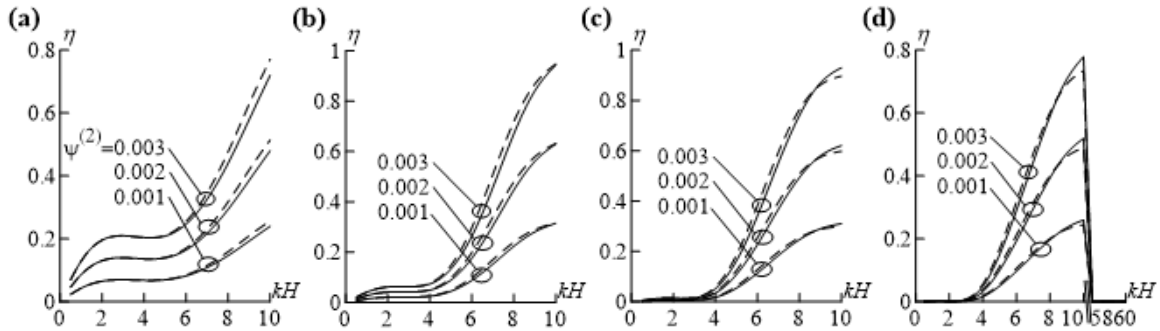

Fig. 26 The influence of the parameter $\psi^{(2)}$ (>0) on the flexural Lamb wave propagation velocity in the second mode for the PZT-2/St/PZT-2 system in the case where $\psi^{(1)}=0$, $a^{(2)}=b^{(2)}=c^{(2)}=0$ and $H_{PZT}/H_{core}=0.5$ (a); $H_{PZT}/H_{core}=1$ (b); $H_{PZT}/H_{core}=2$ (c); $H_{PZT}/H_{core}=4$ (d)

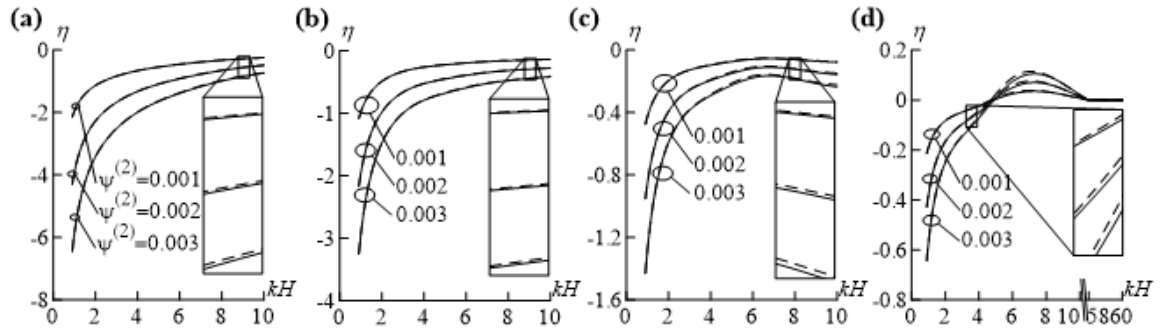

Fig. 27 The influence of the parameter $\psi^{(2)}$ (>0) on the flexural Lamb wave propagation velocity in the second mode for the PZT-2/St/PZT-2 system in the case where $\psi^{(1)}=0$, $a^{(2)}\neq 0$, $b^{(2)}\neq 0$, $c^{(2)}\neq 0$ and $H_{PZT}/H_{core}=0.5$ (a); $H_{PZT}/H_{core}=1$ (b); $H_{PZT}/H_{core}=2$ (c); $H_{PZT}/H_{core}=4$ (d)

Figs. 23 and 26 show that the initial stretching of the core layer under $a^{(2)}=b^{(2)}=c^{(2)}=0$ also causes an increase in the values of the parameter η. However, Figs. 24 and 27 show that in the case where $\psi^{(2)}>0$ and $\psi^{(1)}$ $(=\psi^{(3)})=0$ under $a^{(2)}\neq 0$, $b^{(2)}\neq 0$ and $c^{(2)}\neq 0$ the character of the influence of the initial stress on the wave propagation velocity in the second mode depends on the values of kH.

So, there is a range of change of kH for which the initial stretching of the core layer causes a decrease and there is also a range of change of kH for which the initial stretching causes an increase in the wave propagation velocity in the second mode.

This completes the consideration and analyses of the numerical results.

5. Conclusions

In the present paper the extensional and flexural Lamb waves in the sandwich plate consisting of the pre-stressed piezoelectric face and pre-stressed metal elastic core layers is studied by utilizing the three-dimensional linearized theory of elastic waves in the pre-stressed piezoelectric materials. The solution of the governing field equations for a certain type of piezoelectric material is found. The mechanical relations of the metal elastic core layer material are described through the Murnaghan potential. Dispersion equations for the extensional and flexural Lamb waves are derived for the sufficiently general case. Numerical results on the dispersion of these waves and on the influence of the initial stresses in the constituents of the plate on the wave propagation velocity are presented and discussed.

In these discussions the focus is on the influence of the initial stresses on the extensional and flexural Lamb wave propagation velocities. Numerical results are obtained for the cases where the core layer material is Steel or Aluminum, but the face layers' material is PZT-2 or PZT-6B. Consequently, the sandwich plates PZT-2/St/PZT-2, PZT-2/Al/PZT-2, PZT-6B/St/PZT-6B and PZT-6B/Al/PZT-6B are selected for numerical investigation and it is assumed that on the interface planes between the core and face layers that complete contact conditions are satisfied.

All the numerical results are obtained for the case where the face planes of the piezoelectric layers are electroded and the cases where H_{PZT}/H_{core}=0.5, 1, 2 and 4 are considered. According to these results, the following main conclusions can be drawn:

- The piezoelectricity of the face layers' materials causes the extensional and flexural Lamb waves' propagation velocity to increase.
- The aforementioned increase in the first mode of the Lamb waves is more considerable than in the second mode.
- The initial stretching of the face layers causes an increase in the wave propagation velocity in the first mode and the magnitude of this increase grows with the parameter $\psi^{(1)}$ (30) and with the ratio H_{PZT}/H_{core}, where H_{PZT} is the thickness of the piezoelectric layer and H_{core} is the half thickness of the core layer .
- The piezoelectricity of the face layers' materials causes a decrease in the magnitude of the influence of the initial stretching of the face layers on the wave propagation velocity in the first mode, but in the second mode this influence changes with the values of the dimensionless wavenumber kH .
- The initial stretching (compression) of the core metal layer of the plate under ignoring the third order elastic constants causes an increase (a decrease) in the values of the wave propagation velocity in the first mode. However, the magnitude of this decrease in the case where $\psi^{(2)}<0$ (30) is more significant than the magnitude of the increase in the case where $\psi^{(2)}>0$.
- The magnitude of the influence of the initial stresses in the core layer on the wave propagation velocity decreases with H_{PZT}/H_{core} and increases with the absolute values of $\psi^{(2)}$.
- Taking the third order elastic constants of the metal elastic core layer into consideration

significantly affects the influence of the initial stresses in this layer on the wave propagation velocity in the first mode and this effect has not only a quantitative, but also a qualitative character.

• Taking the third order elastic constants of the metal elastic core layer into consideration there exists such a value of kH (denoted by $(kH)'$) before which (after which), as a result of the initial stretching of the core layer, the wave propagation velocity in the first mode increases (decreases) and in the case where $kH=(kH)'$ the initial stretching of the core layer does not act on the wave propagation velocity.

• Taking the third order elastic constants of the metal elastic core layer into consideration there exists such a value of kH (denoted by $(kH)''$) before which (after which), as a result of the initial compression of the core layer, the wave propagation velocity in the first mode decreases (increases) and in the case where $kH=(kH)''$ the initial compression of the core layer does not act on the wave propagation velocity. It is also established that $(kH)''\approx(kH)'$.

• The influence of the piezoelectricity of PZT-2 on the wave propagation velocities is more significant than that of PZT-6B.

• The initial stretching of the piezoelectric face layers of the plate causes an increase in the wave propagation velocity in the second mode and the character of the influence of the piezoelectricity of the face layers' materials on this increase depends on the values of kH. So, there exists such a value of kH (denote it by (kH^*)) before which (after which) the piezoelectricity causes a decrease (an increase) in the values of the parameter η (30) and the magnitude of this increase grows with kH under $kH>(kH)^*$.

• The initial stretching of the core layer when ignoring the influence of the third order elastic constants causes an increase in the values of the parameter η.

• Taking the influence of the third order elastic constants into account as a result of the initial stretching of the metal elastic core layer, the character of the influence of the initial stress on the wave propagation velocity in the second mode depends on the values of kH. So, there is a range of change of kH for which the initial stretching of the core layer causes a decrease and there is also a range of change of kH for which the initial stretching causes an increase in the values of the wave propagation velocity.

References

Akbarov, S.D. (2015), *Dynamics of Pre-Strained Bi-Material Elastic Systems*, Springer.

Akbarov, S.D., Agasiyev, E.R. and Zamanov, A.D. (2011), "Wave propagation in a pre-strained compressible elastic sandwich plate", *Eur. J. Mech. A-Solid.*, **30**(3), 409-422.

Akbarov, S.D., Kurt, I. and Sezer, S.(2014), "Dispersion of the near-surface waves in a system consisting of a pre-stressed piezoelectric covering layer and a pre-stressed metallic half-plane", *In: Book of abstract of the XVIII conference mechanics of composite materials, Riga, Latvia*, p 23, 2–6 June.

Akbarov, S.D., Zamanov, A.D. and Agasiyev, E.R. (2008) "On the propagation of Lamb waves in a sandwich plate made of compressible materials with finite initial strains", *Mech. Comp. Mater.*, **44**(2), 155–164.

Azrar, L., Belouettar, S. and Wauer, J. (2008), "Nonlinear vibration analysis of actively loaded sandwich piezoelectric beams with geometric imperfections", *Comput. Struct.*, **86**(23), 2182-2191.

Bassiouny, E. (2012), "Thermo-elastic behavior of thin sandwich panel made of piezoelectric layers", *Appl. Math. Comput.*, **218**(20), 10009-10021.

Biot, M. A. (1965), *Mechanics of Incremental Deformation*, Wiley, New York.

Gupta, S., Majhi, D.K., Kundu, S. and Vishwakarma S K. (2012), "Propagation of torsional surface waves in a homogeneous layer of finite thickness over an initially stressed heterogeneous half-space", *Appl. Math. Comput.*, **218**(9), 5655-5664.

Guz, A.N. (2004), *Elastic Waves in Bodies with Initial (Residual) Stresses*, A.C.K., Kiev.

Guz, A.N. and Makhort, F.G. (2000), "The physical fundamentals of the ultrasonic analysis of solids", *Int. Appl. Mech.*, **36**(9), 1119-1148.

Jin, J., Wang, Q. and Quek, S.T. (2002), "Lamb wave propagation in a metallic semi-infinite medium covered with piezoelectric layer", *Int. J. Solids Struct.*, **39**(9), 2547-2556.

Loja, M.A.R., Soares, C.M.M. and Barbosa, J.I. (2013), "Analysis of functionally graded sandwich plate structures with piezoelectric skins, using B-spline finite strip method", *Compos. Struct.*, **96**, 606-615.

Ng, C. T. (2015), "A two-stage approach for quantitative damage imaging in metallic plates using Lamb waves", *Earthq. Struct.*, **8**(4), 821-841.

Pang, Y., Liu, J.X., Wang, Y.S., and Zhao, X.F. (2008), "Propagation of Rayleigh-type surface waves in a transversely isotropic piezoelectric layer on a piezomagnetic half-space", *J. Appl. Phys.*, **103**(7), 074901.

Wang, Q., Yuan, S., Hong, M., and Su, Z. (2015), "On time reversal-based signal enhancement for active lamb wave-based damage identification", *Smart. Struct. Syst.*, **15**(6), 1463-1479.

Yang, J. (2005), *An Introduction to the Theory of Piezoelectricity*, Springer.

CC

Appendix A

In this appendix, we consider the linearized elastic relations for the core layer material. According to the monograph by Guz (2004) and other works listed in the paper by Guz and Mahkort (2000), to obtain results that are consistent with experimental studies of wave propagation patterns of small amplitudes (small perturbations) in compressible metal elastic materials with initial stresses, it is necessary to use the Murnaghan type of elastic potential to describe the linearized elasticity relations of this material. This potential is given as follows (Guz and Makhort 2000)

$$\Phi^{(2)} = \frac{1}{2}\lambda^{(2)}\left(A_1^{(2)}\right)^2 + \mu^{(2)}A_2^{(2)} + \frac{a^{(2)}}{3}\left(A_1^{(2)}\right)^3 + b^{(2)}A_1^{(2)}A_2^{(2)} + \frac{c^{(2)}}{3}A_3^{(2)} \tag{A1}$$

where $\lambda^{(2)}$ and $\mu^{(2)}$ are Lamé constants, $a^{(2)}$, $b^{(2)}$, and $c^{(2)}$ are the third order elasticity constants and $A_1^{(2)}$, $A_2^{(2)}$, and $A_3^{(2)}$ are the first, second, and third algebraic invariants of Green's strain tensor, respectively. For the considered case, the expressions of these invariants are

$$A_1^{(2)} = \varepsilon_{11}^{(2)} + \varepsilon_{22}^{(2)},\ A_2^{(2)} = \left(\varepsilon_{11}^{(2)}\right)^2 + 2\left(\varepsilon_{12}^{(2)}\right)^2 + \left(\varepsilon_{22}^{(2)}\right)^2,$$

$$A_3^{(2)} = \left(\varepsilon_{11}^{(2)}\right)^3 + 3\left(\varepsilon_{12}^{(2)}\right)^2\left(\varepsilon_{11}^{(2)} + \varepsilon_{22}^{(2)}\right) + \left(\varepsilon_{22}^{(2)}\right)^3 \tag{A2}$$

where

$$\varepsilon_{ij}^{(2)} = \frac{1}{2}\left(\frac{\partial u_i^{(2)}}{\partial x_j} + \frac{\partial u_j^{(2)}}{\partial x_i} + \frac{\partial u_n^{(2)}}{\partial x_j}\frac{\partial u_n^{(2)}}{\partial x_i}\right). \tag{A3}$$

The components of the stress tensor are determined through the Murnaghan potential (A1) as follows

$$\sigma_{ij}^{(2)} = \frac{1}{2}\left(\frac{\partial}{\partial \varepsilon_{ij}^{(2)}} + \frac{\partial}{\partial \varepsilon_{ji}^{(2)}}\right)\Phi^{(2)}. \tag{A4}$$

Representing $\sigma_{ij}^{(2)}$, $\varepsilon_{ij}^{(2)}$, and $u_i^{(2)}$ as a summation: $\sigma_{ij}^{(2)} = \sigma_{ij}^{(2),0} + \sigma_{ij}^{(2)\prime}$, $\varepsilon_{ij}^{(2)} = \varepsilon_{ij}^{(2),0} + \varepsilon_{ij}^{(2)\prime}$, and $u_i^{(2)} = u_i^{(2),0} + u_i^{(2)\prime}$, and linearizing the non-linear relations (A3) and (A4) with respect to the perturbations $\sigma_{ij}^{(2)\prime}$, $\varepsilon_{ij}^{(2)\prime}$, and $u_i^{(2)\prime}$, and omitting the prime over these perturbations, we obtain the linearized elasticity relations (4) for the middle layer material, the coefficient of which are determined through the following expressions

$$A_{11}^{(2)} = \lambda^{(2)} + 2\mu^{(2)} + \frac{1}{\mu^{(2)}}(2b^{(2)} + c^{(2)})\sigma_{11}^{(2),0} + \frac{2\sigma_{11}^{(2),0}}{2K_0^{(2)}}\left[\left(a^{(2)} + b^{(2)}\right) - \left(2b^{(2)} + c^{(2)}\right)\frac{\lambda^{(2)}}{2\mu^{(2)}}\right]$$

$$A_{22}^{(2)} = \lambda^{(2)} + 2\mu^{(2)} + \frac{2\sigma_{11}^{(2),0}}{3K_0^{(2)}}\left[\left(a^{(2)} + b^{(2)}\right) - \left(2b^{(2)} + c^{(2)}\right)\frac{\lambda^{(2)}}{2\mu^{(2)}}\right],$$

$$A_{12}^{(2)} = \lambda^{(2)} + \frac{b^{(2)}}{\mu^{(2)}}\sigma_{11}^{(2),0} + \frac{2\sigma_{11}^{(2),0}}{3K_0^{(2)}}\left[\left(a^{(2)} - b^{(2)}\right)\frac{\lambda^{(2)}}{\mu^{(2)}}\right],$$

$$\mu_{12}^{(2)} = \mu^{(2)} + \frac{b^{(2)}\sigma_{11}^{(2),0}}{3K_0^{(2)}} + \frac{c^{(2)}\sigma_{11}^{(2),0}}{4\mu^{(2)}} + \frac{\lambda^{(2)} + 2\mu^{(2)}}{3K_0^{(2)}}\ ,\ K_0^{(2)} = \lambda^{(2)} + \frac{2\mu^{(2)}}{3}. \qquad \text{(A5)}$$

Appendix B

We here give expressions of the functions which enter into Eq. (19).

The case where $c_2^{(1)} < c < c_1^{(1)}$

$$\varphi_{11}(x_2) = \sin(p_1 k x_2),\ \varphi_{12}(x_2) = \cos(p_1 k x_2),\ \varphi_{13}(x_2) = e^{p_2 k x_2},\ \varphi_{14}(x_2) = e^{-p_2 k x_2},$$

$$\varphi_{15}(x_2) = e^{p_3 k x_2},\ \varphi_{16}(x_2) = e^{-p_3 k x_2},\ \varphi_{2i}(x_2) = \alpha_i \varphi_{1i}(x_2),\ \varphi_{3i}(x_2) = \beta_i \varphi_{1i}(x_2),\ i = 1,2,...,6,$$

$$\varphi_{121}(x_2) = (c_{44}^{(1)} p_1 - \alpha_1 c_{44}^{(1)} - \beta_1 e_{15}^{(1)})\cos(p_1 k x_2),\ \varphi_{122}(x_2) = (-c_{44}^{(1)} p_1 - \alpha_2 c_{44}^{(1)} - \beta_2 e_{15}^{(1)})\sin(p_1 k x_2),$$

$$\varphi_{123}(x_2) = (c_{44}^{(1)} p_2 - \alpha_3 c_{44}^{(1)} - \beta_3 e_{15}^{(1)})e^{p_2 k x_2},\ \varphi_{124}(x_2) = (-c_{44}^{(1)} p_2 - \alpha_4 c_{44}^{(1)} - \beta_4 e_{15}^{(1)})e^{-p_2 k x_2},$$

$$\varphi_{125}(x_2) = (c_{44}^{(1)} p_3 - \alpha_5 c_{44}^{(1)} - \beta_5 e_{15}^{(1)})e^{p_3 k x_2},\ \varphi_{126}(x_2) = (-c_{44}^{(1)} p_3 - \alpha_6 c_{44}^{(1)} - \beta_6 e_{15}^{(1)})e^{-p_3 k x_2},$$

$$\varphi_{221}(x_2) = (c_{13}^{(1)} - c_{33}^{(1)}\alpha_1 p_1 - e_{33}^{(1)}\beta_1 p_1)\sin(p_1 k x_2),$$

$$\varphi_{222}(x_2) = (c_{13}^{(1)} + c_{33}^{(1)}\alpha_2 p_1 + e_{33}^{(1)}\beta_2 p_1)\cos(p_1 k x_2),$$

$$\varphi_{223}(x_2) = (c_{13}^{(1)} + c_{33}^{(1)}\alpha_3 p_2 + e_{33}^{(1)}\beta_3 p_2)e^{p_2 k x_2},\ \varphi_{224}(x_2) = (c_{13}^{(1)} - c_{33}^{(1)}\alpha_4 p_2 - e_{33}^{(1)}\beta_4 p_2)e^{-p_2 k x_2},$$

$$\varphi_{225}(x_2) = (c_{13}^{(1)} + c_{33}^{(1)}\alpha_5 p_2 + e_{33}^{(1)}\beta_5 p_3)e^{p_3 k x_2},\ \varphi_{226}(x_2) = (c_{13}^{(1)} - c_{33}^{(1)}\alpha_6 p_2 - e_{33}^{(1)}\beta_6 p_3)e^{-p_3 k x_2},$$

$$\varphi_{41}(x_2) = (e_{31}^{(1)} - e_{33}^{(1)}\alpha_1 p_1 - \varepsilon_{33}^{(1)}\beta_1 p_1)\sin(p_1 k x_2),\ \varphi_{42}(x_2) = (e_{31}^{(1)} + e_{33}^{(1)}\alpha_2 p_1 - \varepsilon_{33}^{(1)}\beta_2 p_1)\cos(p_1 k x_2),$$

$$\varphi_{43}(x_2) = (e_{31}^{(1)} + e_{33}^{(1)}\alpha_3 p_2 - \varepsilon_{33}^{(1)}\beta_3 p_2)e^{p_2 k x_2},\ \varphi_{44}(x_2) = (e_{31}^{(1)} + e_{33}^{(1)}\alpha_4 p_2 - \varepsilon_{33}^{(1)}\beta_4 p_2)e^{-p_2 k x_2},$$

$$\varphi_{45}(x_2) = (e_{31}^{(1)} + e_{33}^{(1)}\alpha_5 p_3 - \varepsilon_{33}^{(1)}\beta_5 p_3)e^{p_3 k x_2},\ \varphi_{46}(x_2) = (e_{31}^{(1)} + e_{33}^{(1)}\alpha_6 p_3 - \varepsilon_{33}^{(1)}\beta_6 p_3)e^{-p_3 k x_2}. \qquad \text{(B1)}$$

The case where $c < c_2^{(1)}$

$$\varphi_{11}(x_2) = e^{p_1 k x_2},\ \varphi_{12}(x_2) = e^{-p_1 k x_2},\ \varphi_{13}(x_2) = e^{p_2 k x_2},\ \varphi_{14}(x_2) = e^{-p_2 k x_2},$$

$$\varphi_{15}(x_2)=e^{p_3kx_2}\varphi_{16}(x_2)=e^{-p_3kx_2},\ \varphi_{2i}(x_2)=\alpha_i\varphi_{1i}(x_2),\ \varphi_{3i}(x_2)=\beta_i\varphi_{1i}(x_2),\ i=1,2,...,6,$$

$$\varphi_{121}(x_2)=(c_{44}^{(1)}p_1-\alpha_1c_{44}^{(1)}-\beta_1e_{15}^{(1)})e^{p_1kx_2},\ \varphi_{122}(x_2)=(-c_{44}^{(1)}p_1-\alpha_2c_{44}^{(1)}-\beta_2e_{15}^{(1)})e^{-p_1kx_2},$$

$$\varphi_{123}(x_2)=(c_{44}^{(1)}p_2-\alpha_3c_{44}^{(1)}-e_{15}^{(1)}\beta_3)e^{p_2kx_2},\ \varphi_{124}(x_2)=(-c_{44}^{(1)}p_2-\alpha_4c_{44}^{(1)}-e_{15}^{(1)}\beta_4)e^{-p_2kx_2},$$

$$\varphi_{125}(x_2)=(c_{44}^{(1)}p_3-\alpha_5c_{44}^{(1)}-e_{15}^{(1)}\beta_5)e^{p_3kx_2},\ \varphi_{126}(x_2)=(-c_{44}^{(1)}p_3-\alpha_6c_{44}^{(1)}-e_{15}^{(1)}\beta_6)e^{-p_3kx_2},$$

$$\varphi_{221}(x_2)=(c_{13}^{(1)}+c_{33}^{(1)}\alpha_1p_1+e_{33}^{(1)}\beta_1p_1)e^{p_1kx_2},\ \varphi_{222}(x_2)=(c_{13}^{(1)}-c_{33}^{(1)}\alpha_2p_1-e_{33}^{(1)}\beta_2p_1)e^{-p_1kx_2},$$

$$\varphi_{223}(x_2)=(c_{13}^{(1)}+c_{33}^{(1)}\alpha_3p_2+e_{33}^{(1)}\beta_3p_2)e^{p_2kx_2},\ \varphi_{224}(x_2)=(c_{13}^{(1)}-c_{33}^{(1)}\alpha_4p_2-e_{33}^{(1)}\beta_4p_2)e^{-p_2kx_2},$$

$$\varphi_{225}(x_2)=(c_{13}^{(1)}+c_{33}^{(1)}\alpha_5p_2+e_{33}^{(1)}\beta_5p_3)e^{p_3kx_2},\ \varphi_{226}(x_2)=(c_{13}^{(1)}-c_{33}^{(1)}\alpha_6p_2-e_{33}^{(1)}\beta_6p_3)e^{-p_3kx_2},$$

$$\varphi_{41}(x_2)=(e_{31}^{(1)}+e_{33}^{(1)}\alpha_1p_1-\varepsilon_{33}^{(1)}\beta_1p_1)e^{p_1kx_2},\ \varphi_{42}(x_2)=(e_{31}^{(1)}-e_{33}^{(1)}\alpha_2p_1+\varepsilon_{33}^{(1)}\beta_2p_1)e^{-p_1kx_2},$$

$$\varphi_{43}(x_2)=(e_{31}^{(1)}+e_{33}^{(1)}\alpha_3p_2-\varepsilon_{33}^{(1)}\beta_3p_2)e^{p_2kx_2},\ \varphi_{44}(x_2)=(e_{31}^{(1)}-e_{33}^{(1)}\alpha_4p_2+\varepsilon_{33}^{(1)}\beta_4p_2)e^{-p_2kx_2},$$

$$\varphi_{45}(x_2)=(e_{31}^{(1)}+e_{33}^{(1)}\alpha_5p_3-\varepsilon_{33}^{(1)}\beta_5p_3)e^{p_3kx_2},\varphi_{46}(x_2)=(e_{31}^{(1)}-e_{33}^{(1)}\alpha_6p_3+\varepsilon_{33}^{(1)}\beta_6p_3)e^{-p_3kx_2}. \quad \text{(B2)}$$

The case where $c>c_1^{(1)}$

$$\varphi_{11}(x_2)=\sin(p_1kx_2),\ \varphi_{12}(x_2)=\cos(p_1kx_2),\ \varphi_{13}(x_2)=\sin(p_2kx_2),\ \varphi_{14}(x_2)=\cos(p_2kx_2),$$
$$\varphi_{15}(x_2)=e^{p_3kx_2},\ \varphi_{16}(x_2)=e^{-p_3kx_2},\ \varphi_{21}(x_2)=\alpha_1\cos(p_1kx_2),\ \varphi_{22}(x_2)=\alpha_2\sin(p_1kx_2),$$

$$\varphi_{23}(x_2)=\alpha_3\cos(p_2kx_2),\ \varphi_{24}(x_2)=\alpha_4\sin(p_2kx_2),\ \varphi_{25}(x_2)=\alpha_5e^{p_3kx_2},\ \varphi_{26}(x_2)=\alpha_6e^{-p_3kx_2},$$
$$\varphi_{31}(x_2)=\beta_1\cos(p_1kx_2),\ \varphi_{32}(x_2)=\beta_2\sin(p_1kx_2),\ \varphi_{34}(x_2)=\beta_3\cos(p_2kx_2),\ \varphi_{35}(x_2)=\beta_5e^{p_3kx_2},$$
$$\varphi_{36}(x_2)=\beta_6e^{-p_3kx_2},\ \varphi_{121}(x_2)=(c_{44}^{(1)}p_1-\alpha_1c_{44}^{(1)}-\beta_1e_{15}^{(1)})\cos(p_1kx_2),$$

$$\varphi_{122}(x_2)=(-c_{44}^{(1)}p_1-\alpha_2c_{44}^{(1)}-\beta_2e_{15}^{(1)})\sin(p_1kx_2),\varphi_{123}(x_2)=(c_{44}^{(1)}p_2-\alpha_3c_{44}^{(1)}-e_{15}^{(1)}\beta_3)\cos(p_2kx_2),$$

$$\varphi_{124}(x_2)=(-c_{44}^{(1)}p_2-\alpha_4c_{44}^{(1)}-e_{15}^{(1)}\beta_4)\sin(p_2kx_2),$$

$$\varphi_{125}(x_2)=(c_{44}^{(1)}p_3-\alpha_5c_{44}^{(1)}-e_{15}^{(1)}\beta_5)e^{p_3kx_2},\ \varphi_{126}(x_2)=(-c_{44}^{(1)}p_3-\alpha_6c_{44}^{(1)}-e_{15}^{(1)}\beta_6)e^{-p_3kx_2},$$

$$\varphi_{221}(x_2)=(c_{13}^{(1)}-c_{33}^{(1)}\alpha_1p_1-e_{33}^{(1)}\beta_1p_1)\sin(p_1kx_2),$$
$$\varphi_{222}(x_2)=(c_{13}^{(1)}+c_{33}^{(1)}\alpha_2p_1+e_{33}^{(1)}\beta_2p_1)\cos(p_1kx_2)$$

$$\varphi_{223}(x_2)=(c_{13}^{(1)}-c_{33}^{(1)}\alpha_3p_2-e_{33}^{(1)}\beta_3p_2)\sin(p_2kx_2),$$
$$\varphi_{224}(x_2)=(c_{13}^{(1)}+c_{33}^{(1)}\alpha_4p_2+e_{33}^{(1)}\beta_4p_2)\cos(p_2kx_2),$$

$$\varphi_{225}(x_2)=(c_{13}^{(1)}+c_{33}^{(1)}\alpha_5p_2+e_{33}^{(1)}\beta_5p_3)e^{p_3kx_2},\ \varphi_{226}(x_2)=(c_{13}^{(1)}-c_{33}^{(1)}\alpha_6p_2-e_{33}^{(1)}\beta_6p_3)e^{-p_3kx_2},$$

$$\varphi_{41}(x_2)=(e_{31}^{(1)}-e_{33}^{(1)}\alpha_1 p_1+\varepsilon_{33}^{(1)}\beta_1 p_1)\sin(p_1 k x_2)\,,\ \varphi_{42}(x_2)=(e_{31}^{(1)}+e_{33}^{(1)}\alpha_2 p_1-\varepsilon_{33}^{(1)}\beta_2 p_1)\cos(p_1 k x_2)\,,$$

$$\varphi_{43}(x_2)=(e_{31}^{(1)}-e_{33}^{(1)}\alpha_3 p_2+\varepsilon_{33}^{(1)}\beta_3 p_2)\sin(p_2 k x_2)\,,$$

$$\varphi_{44}(x_2)=(e_{31}^{(1)}+e_{33}^{(1)}\alpha_4 p_2-\varepsilon_{33}^{(1)}\beta_4 p_2)\cos(p_2 k x_2)\,,$$

$$\varphi_{45}(x_2)=(e_{31}^{(1)}+e_{33}^{(1)}\alpha_5 p_3-\varepsilon_{33}^{(1)}\beta_5 p_3)e^{p_3 k x_2}\,,\ \varphi_{46}(x_2)=(e_{31}^{(1)}-e_{33}^{(1)}\alpha_6 p_3+\varepsilon_{33}^{(1)}\beta_6 p_3)e^{-p_3 k x_2}\,. \quad \text{(B3)}$$

Substituting the expressions for $u_1^{(1)}$, $u_2^{(1)}$, and $\varphi^{(1)}$ in (B1)-(B3) into the equation of motion (12), we can easily determine the values of the constants α_1, α_2,…, α_6 and the values of the constants $\beta_1, \beta_2, \ldots, \beta_6$ which enter the foregoing expressions in (B1)-(B3).

Appendix C

The equations obtained from the contact and boundary conditions (6)-(11) for the extensional Lamb waves, i.e., for the cases where the condition (26) is satisfied, are

$$u_1^{(1)}\Big|_{x_2=h_1}-u_1^{(2)}\Big|_{x_2=h_1}=\sum_{i=1}^{6}A_i\varphi_{1i}(kh_1)\ -Z_2G_2\cosh(R_1kh_1)-Z_4G_4\cosh(R_2kh_1)=0\,,$$

$$u_2^{(1)}\Big|_{x_2=h_1}-u_2^{(2)}\Big|_{x_2=h_1}=\sum_{i=1}^{6}A_i\varphi_{2i}(kh_1)\ -Z_2\sinh(R_1kh_1)\ -Z_4\sinh(R_2kh_1)=0\,,$$

$$\sigma_{12}^{(1)}\Big|_{x_2=h_1}=\sigma_{12}^{(2)}\Big|_{x_2=h_1}\ \Rightarrow\sum_{i=1}^{6}A_i\varphi_{12i}(kh_1)$$

$$-Z_2\mu_{12}\left(G_2R_1-1\right)\sinh(R_1kh_1)-Z_4\mu_{12}\left(G_4R_2-1\right)\sinh(R_2kh_1)=0,$$

$$\sigma_{22}^{(1)}\Big|_{x_2=h_1}=\sigma_{22}^{(2)}\Big|_{x_2=h_1}\ \Rightarrow\sum_{i=1}^{6}A_i\varphi_{22i}(kh_1)$$

$$-Z_2\left(A_{12}G_2+A_{22}R_1\right)\cosh(R_1kh_1)-Z_4\left(A_{12}G_4+A_{22}R_2\right)\cosh(R_2kh_1)=0,$$

$$\varphi^{(1)}\Big|_{x_2=h_1}=0\ \Rightarrow\sum_{i=1}^{6}A_i\varphi_{3i}(kh_1)=0\qquad\text{(for an electroded case),}$$

$$D_2\big|_{x_2=h_1}=0\ \Rightarrow\sum_{i=1}^{6}A_i\varphi_{4i}(kh_1)\qquad\text{(for an unelectroded case).}$$

$$\sigma_{12}^{(1)}\Big|_{x_2=h_2}=0\ \Rightarrow\sum_{i=1}^{6}A_i\varphi_{12i}(kh_2)=0\,,\ \sigma_{22}^{(1)}\Big|_{x_2=h_2}=0\ \Rightarrow\sum_{i=1}^{6}A_i\varphi_{22i}(kh_2)=0\,,$$

$$\varphi^{(1)}\Big|_{x_2=h_2}=0 \;\Rightarrow \sum_{i=1}^{6} A_i\varphi_{3i}(kh_2)=0 \text{ (for a short circuit case),}$$

$$D_2^{(1)}\Big|_{x_2=h_2}=0 \;\Rightarrow \sum_{i=1}^{6} A_i\varphi_{4i}(kh_2)=0 \text{ (for an open circuit case).} \qquad \text{(C1)}$$

The first four equations obtained from the contact and boundary conditions (6)-(11) for the flexural Lamb waves, i.e., for the cases where the condition (27) is satisfied, are

$$u_1^{(1)}\Big|_{x_2=h_1}-u_1^{(2)}\Big|_{x_2=h_1}=\sum_{i=1}^{6} A_i\varphi_{1i}(kh_1)\;-Z_1G_2\sinh(R_1kh_1)\;-Z_3G_4\sinh(R_2kh_1)=0\,,$$

$$u_2^{(1)}\Big|_{x_2=h_1}-u_2^{(2)}\Big|_{x_2=h_1}=\sum_{i=1}^{6} A_i\varphi_{2i}(kh_1)\;-Z_1\cosh(R_1kh_1)\;-Z_3\cosh(R_2kh_1)=0\,,$$

$$\sigma_{12}^{(1)}\Big|_{x_2=h_1}=\sigma_{12}^{(2)}\Big|_{x_2=h_1} \;\Rightarrow \sum_{i=1}^{6} A_i\varphi_{12i}(kh_1)$$

$$-Z_1\mu_{12}\left(G_2R_1-1\right)\cosh(R_1kh_1)-Z_3\mu_{12}\left(G_4R_2-1\right)\cosh(R_2kh_1)=0,$$

$$\sigma_{22}^{(1)}\Big|_{x_2=h_1}=\sigma_{22}^{(2)}\Big|_{x_2=h_1} \;\Rightarrow \sum_{i=1}^{6} A_i\varphi_{22i}(kh_1)$$

$$-Z_1\left(A_{12}G_2+A_{22}R_1\right)\sinh(R_1kh_1)-Z_3\left(A_{12}G_4+A_{22}R_2\right)\sinh(R_2kh_1)=0\,. \qquad \text{(C2)}$$

Note that the remaining six equations obtained for the flexural Lamb waves coincide with the last six equations given in (C1).